Article

Metallacarbenes from Diazoalkanes: An Experimental and Computational Study of the Reaction Mechanism

Revital Cohen, Boris Rybtchinski, Mark Gandelman, Haim Rozenberg, Jan M. L. Martin, and David Milstein

J. Am. Chem. Soc., **2003**, 125 (21), 6532-6546• DOI: 10.1021/ja028923c • Publication Date (Web): 01 May 2003

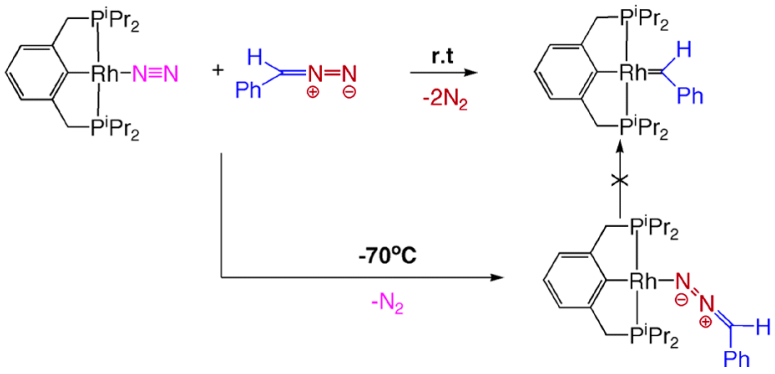

More About This Article

Additional resources and features associated with this article are available within the HTML version:

- Supporting Information
- Links to the 16 articles that cite this article, as of the time of this article download
- Access to high resolution figures
- Links to articles and content related to this article
- Copyright permission to reproduce figures and/or text from this article

View the Full Text HTML

J|A|C|S
ARTICLES
Published on Web 05/01/2003

Metallacarbenes from Diazoalkanes: An Experimental and Computational Study of the Reaction Mechanism

Revital Cohen, Boris Rybtchinski, Mark Gandelman, Haim Rozenberg, Jan M. L. Martin,* and David Milstein*

Contribution from the Department of Organic Chemistry, The Weizmann Institute of Science, 76100 Rehovot, Israel

Received October 13, 2002; E-mail: david.milstein@weizmann.ac.il; comartin@wicc.weizmann.ac.il

Abstract: PCP ligand (1,3-bis-[(diisopropyl-phosphanyl)-methyl]-benzene), and PCN ligand ({3-[(di-*tert*-butyl-phosphanyl)-methyl]-benzyl}-diethyl-amine) based rhodium dinitrogen complexes (**1** and **2**, respectively) react with phenyl diazomethane at room temperature to give PCP and PCN−Rh carbene complexes (**3** and **5**, respectively). At low temperature (−70 °C), PCP and PCN phenyl diazomethane complexes (**4** and **6**, respectively) are formed upon addition of phenyl diazomethane to **1** and **2**. In these complexes, the diazo moiety is η^1 coordinated through the terminal nitrogen atom. Decomposition of complexes **4** and **6** at low temperatures leads only to a relatively small amount of the corresponding carbene complexes, the major products of decomposition being the dinitrogen complexes **1** and **2** and stilbene. This and competition experiments (decomposition of **6** in the presence of **1**) suggests that phenyl diazomethane can dissociate under the reaction conditions and attack the metal center through the diazo carbon producing a η^1-C bound diazo complex. Computational studies based on a two-layer ONIOM model, using the mPW1K exchange-correlation functional and a variety of basis sets for PCP based systems, provide mechanistic insight. In the case of less bulky PCP ligand bearing H-substituents on the phosphines, a variety of mechanisms are possible, including both dissociative and nondissociative pathways. On the other hand, in the case of i-Pr substituents, the η^1-C bound diazo complex appears to be a critical intermediate for carbene complex formation, in good agreement with the experimental results. Our results and the analysis of reported data suggest that the outcome of the reaction between a diazoalkane and a late transition metal complex can be anticipated considering steric requirements relevant to η^1-C diazo complex formation.

Introduction

Diazoalkanes represent a very important class of reagents in organometallic chemistry[1−3] regarding metallacarbene synthesis,[1,4,5] cyclopropanation,[6] and C−H bond activation.[6, 7] Metal-mediated synthesis of reactive I, N, S, Se, and O ylides using diazoalkanes is also of significant synthetic value.[8]

Transition metal complex mediated cyclopropanation of olefins using diazoesters is among the best methods for the synthesis of cyclopropane derivatives.[6] Computational studies regarding various aspects of diazoalkane reactivity in transition metal chemistry have been reported.[9] Intramolecular C−H bond activation in diazoesters promoted by Rh(II) complexes has been utilized for the construction of medium size rings.[6] Recently, catalytic *intermolecular* C−H activation of alkanes with diazoacetates has been reported.[7] Metallacarbenes are thought to be the reactive intermediates in both cyclopropanation and C−H bond activation.[6,7]

Two important early discoveries introduced diazo compounds into synthetic organometallic chemistry as useful reagents for metal carbene synthesis. Herrmann utilized diazo compounds as versatile carbene synthons in the case of unsaturated manganese complexes,[10] and Roper employed diazomethane in the synthesis of Ru and Os carbenes, which were found to be stable, isolable compounds.[4,11] Nowadays, the synthesis of late transition metal carbenes relies extensively on the use of diazoalkanes. Grubbs et al. have synthesized a variety of Ru carbenes using diazoalkanes,[12] including $(PCy_3)_2Cl_2Ru{=}CH$-

(1) Herrmann, W. A. *Angew. Chem., Int. Ed. Engl.* **1978**, *17*, 800.
(2) Mizobe, Y.; Ishii, Y.; Hidai, M. *Coord. Chem. Rev.* **1995**, *139*, 281.
(3) Putala, M.; Lemenovskii, D. A. *Russ. Chem. Rev.* **1994**, *63*, 197.
(4) Roper, W. R. *J. Organomet. Chem.* **1986**, *300*, 167.
(5) Werner, H. *J. Organomet. Chem.* **1995**, *500*, 331.
(6) (a) Padwa, A.; Weingarten, M. D. *Chem. Rev.* **1996**, *96*, 223. (b) Doyle, M. P.; Forbes, D. C. *Chem. Rev.* **1998**, *98*, 911. (c) Davies, H. M. L.; Panaro, S. A. *Tetrahedron* **2000**, *56*, 4871.
(7) For a recent review on intermolecular C−H activation see: Davies, H. M. L.; Antoulinakis, E. G. *J. Organomet. Chem.* **2001**, *617*−*618*, 47.
(8) For a recent review, see: Hodgson, D. M.; Pierard, F. Y. T. M.; Stupple, P. A. *Chem. Soc. Rev.* **2001**, *30*, 50.
(9) For recent theoretical works, see: (a) A review on transition metal-main group multiple bonding: Cundari, T. R. *Chem. Rev.* **2000**, *100*, 807. (b) Diazoalkanes in the metal catalyzed formation of carbonyl and ammonium ylides: Padwa, A.; Snyder, J. P.; Curtis, E. A.; Sheehan, S. M.; Worsencroft, K. J.; Kappe, C. O. *J. Am. Chem. Soc.* **2000**, *122*, 8155. (c) Cyclopropanation: Bernardi, F.; Bottoni, A.; Miscione, G. P. *Organometallics* **2001**, *20*, 2751; Rodriguez-Garcia, C.; Oliva, A.; Ortuno, R.; Branchadell, V. *J. Am. Chem. Soc.* **2001**, *123*, 6157. (d) C−H bond activation: Nakamura, E.; Yoshikai, M.; Yamanaka, M. *J. Am. Chem. Soc.* **2002**, *124*, 7181.
(10) (a) Herrmann, W. A. *Angew. Chem., Int. Ed. Engl.* **1974**, *13*, 639. (b) Herrmann, W. A. *Chem. Ber.* **1975**, *108*, 486.
(11) Hill, A. F.; Roper, W. R.; Waters, J. M.; Wright, A. H. *J. Am. Chem. Soc.* **1983**, *105*, 3939.
(12) (a) Schwab, P.; France, M. B.; Ziller, J. W.; Grubbs, R. H. *Angew. Chem., Int. Ed. Engl.* **1995**, *34*, 2039. (b) Schwab, P.; Grubbs, R. H.; Ziller, J. W. *J. Am. Chem. Soc.* **1996**, *118*, 100. (c) Sanford, M. S.; Valdez, M. R.; Grubbs, R. H. *Organometallics* **2001**, *20*, 5455.

10.1021/ja028923c CCC: $25.00

Scheme 1

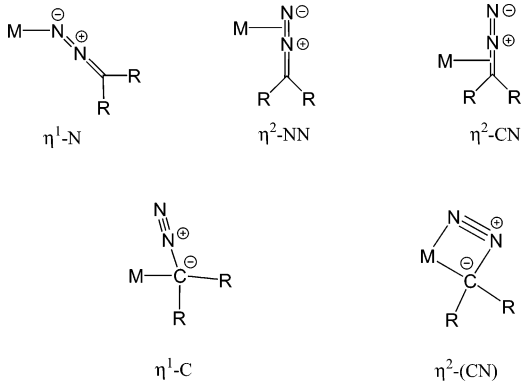

(Ph) which was synthesized by using phenyl diazomethane.[13] This compound and its derivatives are widely used as very efficient metathesis catalysts in organic synthesis and polymer science. In seminal work on the synthesis of late transition metal carbenes by Werner, diazoalkanes are also widely utilized as carbene precursors. [5,14,15] It was demonstrated that careful choice of the ligands and the diazo compounds is critical for the carbene synthesis.[5,14] In some catalytic cyclopropanation systems utilizing diazo compounds, various carbene complexes have been isolated.[16] We have recently reported the synthesis of a PCP−Rh carbene complex using $PhCHN_2$.[17]

Metallacarbenes are not always the products of the reaction of a transition metal complex with a diazo compound. A significant number of stable diazoalkane complexes have been isolated in the reaction of certain transition metal complexes with diazoalkanes.[2,18] The coordination modes of diazoalkanes, displayed at mono- and multimetallic centers, are quite diverse. Monometallic complexes reported to date include either η^2-diazoalkane ligands bound through the N−N multiple bonds (η^2-NN)[2,18,19] or η^1-diazoalkane ligands coordinated at the terminal nitrogen atom (η^1-N)[2,5,18,20] (Scheme 1). Other possible coordination modes of diazoalkane ligands include η^2-binding through the C−N bond (η^2-CN), the four-membered ring cycloadduct (η^2-(CN)), and coordination through the carbon atom (η^1-C). However, unambiguous examples of these types are yet unknown, although complexes of the type η^1-C are frequently assumed to be the initial intermediates preceding metallacarbene species formation in the transition-metal-catalyzed carbenoid reactions using diazoalkanes.[21]

No examples of an η^2 coordination mode through the C−N bond as well as an η^2-(CN) cycloadduct have yet been reported. As described before, reactions of diazoalkanes with metal complexes often result in the formation of metallacarbenes and liberation of N_2. As a result, only a few examples where well-defined diazoalkane complexes undergo clean N_2 loss to give carbene complexes are known. In a review on the synthesis and reactivity of diazoalkane complexes, Hidai pointed out that in the course of carbene formation, "the coordination of a diazoalkane to a metal complex precedes the N_2 loss from the diazoalkane, and it is of great importance to elucidate how the N_2 extrusion from the diazoalkane ligands proceeds in these complexes".[2] In general, the reaction aptitudes of diazoalkanes toward metal centers are not well understood, and the intimate mechanism of the carbene formation from the diazo compounds has not been investigated experimentally. Factors controlling formation of metal carbenes from diazoalkanes are not well understood and the rational choice of ligands, diazoalkanes, and reaction conditions remains a significant challenge in metallacarbene synthesis.

Here, we report an experimental and computational study on metallacarbene formation using a diazoalkane (phenyl diazomethane) as a carbene donor. The phenyl diazomethane complex observed at the initial stages of reaction appears to be a side equilibrium compound rather than a true intermediate in the process of the carbene complex formation. We show that the key intermediate on the pathway of metallacarbene formation is a complex with a diazoalkane carbon atom (η^1-C) rather than a nitrogen atom bound to the metal center. We suggest that the outcome of the reaction between a diazoalkane and a late transition metal complex can be anticipated using simple electronic and steric arguments, and propose a generalization of the known reactivity patterns.

Results

A. Experimental Results. Continuing our studies on PCP[22] and PCN-type[23] complexes we became interested in the mechanism of carbene complex formation from the corresponding PCP and PCN type rhodium dinitrogen complexes and $PhCHN_2$. The rigid chelating PCP and PCN frameworks enhances complex stability and introduces a range of special properties, providing models for mechanistic studies and efficient catalysts.[24]

PCP and PCN−Rh Dinitrogen Complexes. The PCP dinitrogen complex **1** was synthesized as described in Scheme 2. The analogous PCN complex **2** was prepared by reacting the corresponding methyl chloride complex with $NaHBEt_3$ (see the Experimental section). These complexes exist as mixtures of monomer (**1a**, **2a**) and dimer (**1b**, **2b**) species, in a ratio which depends on the concentration of the complexes and N_2. Thus, bubbling with argon or freeze−pump−thaw cycles accompanied

(13) For recent reviews, see: (a) Trnka, T. M.; Grubbs R. H. *Acc. Chem. Res.* **2001**, *34*, 18. (b) Fürstner, A. *Angew. Chem., Int. Ed. Engl.* **2000**, *39*, 3012.
(14) (a) Werner, H.; Schwab, P.; Bleuel, E.; Mahr, N.; Steinert, P.; Wolf, *Chem. Eur. J.* **1997**, *3*, 1375. (b) Ortmann, D. A.; Weberndorfer, B.; Ilg, K.; Laubender, M.; Werner, H. *Organometallics* **2002**, *21*, 2369.
(15) (a) Weberndörfer, B.; Henig, G.; Werner, H. *Organometallics* **2000**, *19*, 4687. (b) Werner, H.; Stüer, W.; Wolf, J.; Laubender, M.; Weberndörfer, B.; Herbst-Irmer, R.; Lehmann C. *Chem. Eur. J.* **1999**, *11*, 1889. (c) Werner, H.; Stüer, W.; Weberndörfer, B.; Wolf, J. *Chem. Eur. J.* **1999**, *10*, 1707.
(16) For recent examples, see: (a) Galardon, E.; Le Maux, P.; Toupet, L.; Simonneaux G. *Organometallics* **1998**, *17*, 565. (b) Lee, H. M.; Bianchini, C.; Jia, G.; Barbaro, P. *Organometallics* **1999**, *18*, 1961.
(17) Vigalok, A.; Milstein, D. *Organometallics* **2000**, *19*, 2061.
(18) (a) Sutton, D. *Chem. Rev.* **1993**, *93*, 995. (b) Dartiguenave, M.; Menu, M. J.; Deydier, E.; Dartiguenave, Y.; Siebald, H. *Coord. Chem. Rev.* **1998**, *178−180*, 623.
(19) (a) Polse, J. L.; Kaplan, A. W.; Andersen, R. A.; Bergman, R. G. *J. Am. Chem. Soc*. **1998**, *120*, 6316. (b) Polse, J. L.; Andersen, R. A.; Bergman, R. G. *J. Am. Chem. Soc.* **1996**, *118*, 8737. (c) Kaplan, A. W.; Polse, J. L.; Ball, G. E.; Andersen, R. A.; Bergman, R. G. *J. Am. Chem. Soc.* **1998**, *120*, 11 649.
(20) Albertin, G.; Antoniutti, S.; Bordignon, E.; Carrera, B. *Inorg. Chem*. **2000**, *39*, 4646.
(21) (a) Maxwell, J. L.; Brown, K. C.; Bartley, D.; Kodadek T. *Science* **1992**, *256*, 1544. (b) Bartley, D.; Kodadek T. *J. Am. Chem. Soc*. **1993**, *115*, 1656.
(22) For example: (a) Ohff, M.; Ohff, A.; van der Boom, M. E.; Milstein, D. *J. Am. Chem. Soc.* **1997**, *119*, 11 687. (b) Vigalok, A.; Uzan, O.; Shimon, L. J. W.; Ben-David, Y.; Martin, J. M. L.; Milstein, D. *J. Am. Chem. Soc.* **1998**, *120*, 12 539. (c) Cohen, R.; van der Boom, M. E.; Shimon, L. J. W.; Rozenberg, H.; Milstein, D. *J. Am. Chem. Soc.* **2000**, *122*, 7723.
(23) (a) Gandelman, M.; Vigalok, A.;. Shimon, L. J. W.; Milstein, D. *Organometallics* **1997**, *16*, 3981. (b) Gandelman, M.; Vigalok, A.;. Konstantinovski, L.; Milstein, D. *J. Am. Chem. Soc.* **2000**, *122*, 9848. (c) Gandelman, M.; Milstein, D. *Chem. Commun.* **2000**, 1603.
(24) Reviews: (a) Rybtchinski, B.; Milstein, D. *Angew. Chem., Int. Ed. Engl.* **1999**, *38*, 870. (b) Jensen, C. M. *Chem. Comm*. **1999**, 2443. (c) Albrecht, M.; van Koten, G. *Angew. Chem., Int. Ed. Engl.* **2001**, *40*, 3750. (d) Vigalok A, Milstein D. *Acc. Chem. Res.* **2001**, *34*, 798.

Scheme 2

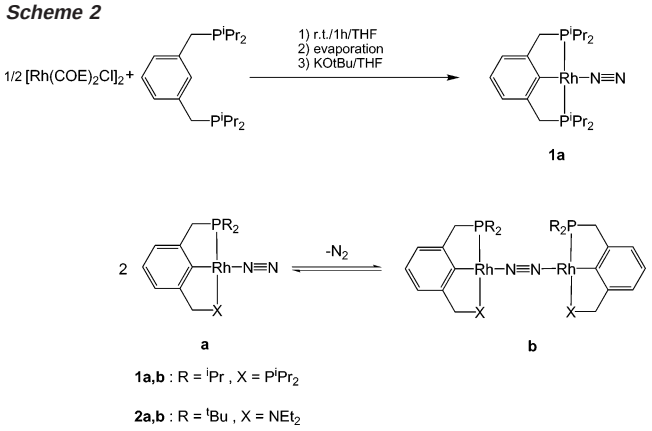

with argon refill resulted in almost exclusive formation of the dimers **1b** and **2b**. At the typical concentrations of the experiment (~0.4M) under 1atm. N_2 at room temperature, the following ratios are observed: **1a**:**1b** = 8:3, **2a**:**2b** = 3:7; at −50 °C **1a**:**1b** = 1:1, **2a**:**2b** = 1:2. These ratios are most probably determined by a balance of steric and electronic factors. Similar dimer-monomer equilibria in the case of various dinitrogen complexes have been reported.[25,26] For the sake of simplicity, we depict complexes **1** and **2** as the monomers in all the schemes, although dimer species are present. Crystals of **1b** suitable for X-ray analysis were grown at −35 °C from a toluene-pentane solution of **1a,b**. Only **1b** crystallizes under these conditions. The X-ray structure of **1b** reveals that the dinitrogen molecule is bridging between two square planar PCP−Rh units, which are twisted around the RhNNRh axis with a dihedral angle of 33(4)° (Figure 1). The coordinated dinitrogen molecule is not activated, the N−N bond length (1.108(3) Å) being close to the one in free N_2.

PCP System: Carbene and Diazoalkane Complex Formation. When complex **1** is reacted at room temperature with 1 equiv of $PhCHN_2$ in benzene, N_2 evolution takes place and formation of the carbene complex **3** is observed (Scheme 3). Preparation of this complex using a sulfur ylide precursor has been recently reported by us.[27] When an equimolar amount of $PhCHN_2$ is added to complex **1** at −70 °C in toluene the dark green diazo complex **4** is formed quantitatively. It was characterized by multinuclear NMR at −60 °C. Complex **4** gives rise to a doublet at 66.46 ppm ($^1J_{RhP}$ = 154.4 Hz) in $^{31}P\{^1H\}$ NMR. The Rh atom is bound to the aryl ring of the ligand as evident from the splitting pattern of the ipso carbon in the ^{13}C NMR spectrum, which appears as a doublet of triplets centered at 173.02 ppm ($^1J_{RhC}$ = 38.3 Hz, $^2J_{PC}$ = 4.9 Hz). The signal of the Ph*CH*N_2 group appears in the ^1H NMR spectrum as a singlet centered at 3.76 ppm, the chemical shift being similar to the reported one (4.13 ppm) for a $PhCHN_2$−Rh complex.[28] In the ^{13}C NMR spectrum, the coordinated Ph*CH*N_2 gives rise to a singlet at 57.95 ppm, ruling out the η^1-C coordination mode (see Scheme 1). Coordination through the terminal N atom (end-on η^1-N mode) of the diazoalkane was confirmed by a

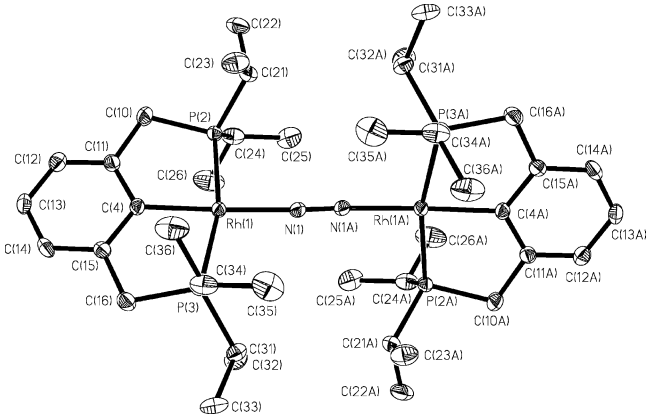

Figure 1. ORTEP plot of the X-ray structure of **1b**. Hydrogen atoms are omitted for clarity. Selected bond lengths (Å) and bond angles (degrees): N(1)−N(1A) = 1.108(3), Rh(1)−N(1) = 1.9687(17), Rh(1)−C(4) = 2.039-(2), Rh(1)−P(2) = 2.2680(9), Rh(1)−P(3) = 2.2688(8); Rh(1)−N(1)−N(1A) = 177.3(2), C(4)−Rh(1)−N(1) = 178.18(7), P(2)−Rh(1)−N(1) = 95.25(5), P(3)−Rh(1)−N(1) = 98.70(5), P(2)−Rh(1)−P(3) = 165.82(2), C(4)−Rh(1)−P(2) = 83.10(6), C(4)−Rh(1)−P(3) = 82.92(7); Rh(1)−N(1)−N(1A)−Rh(1A) = −147(4); C(4)−Rh(1)−N(1)−N(1A) = −11(4).

Scheme 3

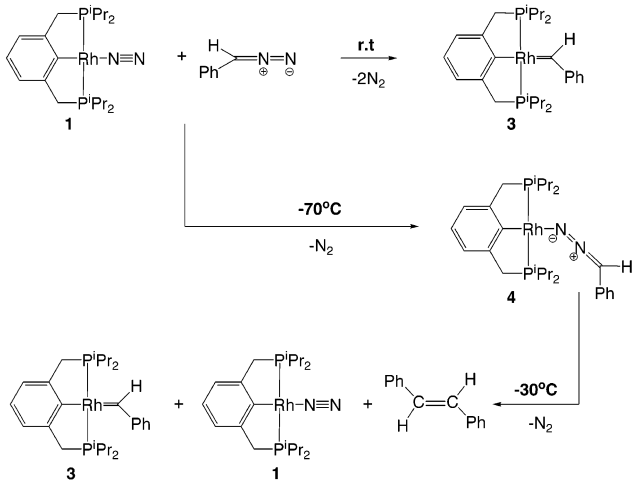

heteronuclear 2D ^{15}N-^1H correlation experiment. In the correlation spectrum, two ^{15}N cross-peaks (related to a Ph*CH*N_2 hydrogen signal) appear: a doublet centered at 421.77 ppm ($^1J_{RhN}$ = 31.5 Hz, Rh-*N*≡NCHPh), and a singlet at 300.03 ppm (Rh−N≡*N*CHPh).[29] Surprisingly, when heated to 30 °C, complex **4** does not convert cleanly to the rhodium carbene **3**, but gives only 30% of **3**, the other products being the Rh nitrogen complexes **1** and stilbene. Formation of the carbene complex was observed to start at −50 °C, the process being very slow. It should be noted that when an *excess* of $PhCHN_2$ is added to the carbene complex at −70 °C and the solution slowly warmed, stilbene formation starts to take place at −50 °C (the temperature at which the *carbene formation was observed to begin*), concurrently with formation of the dinitrogen complex. Stilbene can be formed also in the process of carbene decompostion (probably by dimerization); however, at room temperature this process was observed to proceed for hours and does not occur at all at −50 °C. Thus, stilbene formation can be explained by the reaction of the diazoalkane with the carbene

(25) (a) van der Boom, M. E.; Liou, Sh.-Y.; Ben-David, Y.; Shimon, L. J. W.; Milstein D. *J. Am. Chem. Soc*. **1998**, *120*, 6531. (b) Gusev, D. G.; Dolgushin, F. M.; Antipin, M. Yu. *Organometallics* **2000**, *19*, 3429.
(26) Yoshida, T.; Okano, T.; Thorn, D. L.; Tulip, T. H.; Otsuka S.; Ibers, J. A. *J. Organomet. Chem.* **1979**, *181*, 183.
(27) Gandelman, M.; Rybtchinski, B.; Ashkenazi, N.; Gauvin, R.; Milstein D. *J. Am. Chem. Soc*. **2001**, *123*, 5372.
(28) Werner, H.; Mahr, N.; Frenking, G.; Jonas, V. *Organometallics* **1995**, *14*, 619.
(29) For the ^{15}N NMR data of the diazo compounds, see: Regitz, M.; Maas, G. *Diazo Compounds Properties and Synthesis*; Academic Press Inc.: New York, 1986, pp 47−56.

Scheme 4

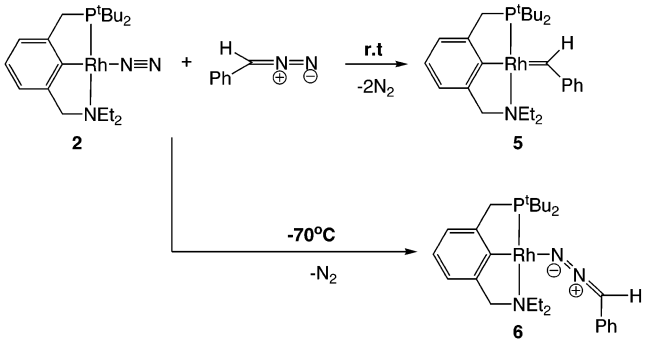

complex. We suggest that as the rate of formation of the carbene complex **3** is decreased at low temperatures and the lifetime of the diazoalkane complex **4** is increased, the concentration of free $PhCHN_2$ formed by dissociation from **4** is sufficient for significant carbene consumption. An intermolecular reaction between bound diazoalkane and the carbene complex is also a possibility, although it seems less probable due to steric factors (see below).

Thus, there is a striking difference between the reaction of $PhCHN_2$ with **1** at room temperature and at low temperatures. The end-on η^1-N diazo complex decomposition does not lead to clean carbene formation, in line with previous observations that diazo complexes may resist N_2 loss and hamper carbene formation.[2,3]

PCN System: Carbene and Diazo Complex Formation. The PCN−Rh carbene **5** was quantitatively formed by reaction of the dinitrogen complex **2** with $PhCHN_2$ at room temperature, analogously to formation of the PCP−Rh complex **3** (Scheme 4). Preparation of complex **5** by the sulfur ylide method was recently reported by us.[27] Analogously to the PCP system, when an equimolar amount of $PhCHN_2$ is added to complex **2** at −70 °C in toluene, the dark green diazoalkane complex **6** is formed quantitatively. Complex **6** gives rise to a doublet at 88.90 ppm ($^1J_{RhP}$ = 204.6 Hz) in $^{31}P\{^1H\}$ NMR. The signals of the Ph*CH*N_2 group appear in the ^1H NMR spectrum as a singlet centered at 3.84 ppm and in the ^{13}C NMR as a singlet at 68.89 ppm. Formation of the carbene complex **5** from **6** was observed to start at −50 °C. At this temperature and at higher temperatures complex **6** decomposes to give the dinitrogen complex **2** along with unidentified products, and *only a small amount of the carbene complex **5** is observed*, in a sharp contrast to the reaction at room temperature. Stilbene formation along with unidentified organic products was observed.

Possible Pathways for Carbene Complex Formation. Three distinct pathways for carbene complex formation can be envisaged (Scheme 5). In pathway I, (the intramolecular "bound diazo" mechanism), the end-on diazo transforms into the carbene complex without detachment, i.e., it is bound to the metal center throughout the reaction sequence. In pathway II (the intermolecular "direct attack" mechanism), $PhCHN_2$ dissociates from the metal center and then attacks it via the diazo carbon. In pathway III (the "bimolecular" mechanism), bound diazoalkane reacts with the metal center of another complex which could be a complex of diazoalkane, dinitrogen, or a T-shaped 14e intermediate. Unfortunately, the kinetic follow-up of the decomposition of the diazoalkane complexes **4** and **6** was hampered by a significant overlap between the signals of **1** and **4** in $^{31}P\{^1H\}$ and ^1H NMR and by an unclean reaction in the case of **6**. To explore the above-mentioned pathways (I−III), we performed competition experiments, designed to probe the possibility of diazoalkane detachment from the metal center.

Competition Experiments. Complex **6** was obtained at −78 °C, as described above, and the dinitrogen PCP complex **1** was added to it at −78 °C (Scheme 6). The solution containing a mixture of **6** and **1** (**6**:**1** = 1:2) was placed in an NMR probe pre-cooled to −70 °C. No reaction took place at this temperature, the ratio remaining the same for hours. When heated to −50 °C slow formation of *both PCP and PCN carbene complexes **3** and **5*** was observed. Keeping the solution overnight at −50 °C resulted in a mixture containing the carbene complexes **3** and **5,** the PCP dinitrogen complex **1** and the PCN dinitrogen complex **2** (about 50% conversion, **3**:**5** = 6:5). A small amount of the PCP diazo complex **4** (3−4%) was also observed.

In another experiment, a mixture of **1** and **6** (**6**:**1** = 1:2) was prepared at −78 °C in toluene and placed in an NMR probe pre-cooled to −70 °C. It was then heated to 0 °C, upon which immediate formation of the carbene complexes **3** and **5** took place, resulting in a ratio **3**:**5** = 3:4 as observed by ^{31}P and ^1H NMR. This ratio changed only slightly at 0 °C for hours, due to slow carbene decomposition to produce the corresponding dinitrogen complexes and stilbene. In the experiments described above no carbene transfer from **5** to **1** took place neither at −50 °C nor at 0 °C.

Thus, formation of both PCP and PCN carbenes **3** and **5** (which do not interconvert at the given temperature and do not undergo carbene transfer) starting from the PCN diazoalkane complex **6** suggests that the *diazoalkane can detach from the metal center* (pathway II). The possibility of the *bimolecular mechanism* (pathway III, see Scheme 5), that can lead to the same observations as for the pathway II, cannot be ruled out. However, the following reasons suggest that it is less probable than II: (1) decomposition of **4** was observed to start at the same facility independent of its concentration (inconsistent with pathway IIIA); (2) decomposition of **6** is not increased significantly upon addition of a 2-fold access of the dinitrogen complex **1** (inconsistent with pathways IIIB and IIIC); (3) a small amount of the PCP diazo complex **4** is formed at low temperatures upon mixing **6** and **1**, indicating that $PhCHN_2$ dissociates from **6** and is trapped by **1**. For further clarification concerning pathway III see the Computational Results section.

B. Computational Results. To clarify the reaction mechanism, Density Functional Theory (DFT) calculations were performed. Calculations were carried out first for the PCP system with H substituents on the phosphines (H−PCP system) and CH_2N_2 instead of $PhCHN_2$ in order to reduce the computation time. Afterward, the calculations were performed for the H−PCP−Rh/$PhCHN_2$ system to identify plausible reaction pathways. Finally, ^{i}Pr groups were introduced in an ONIOM[30] approach to obtain a computational description (^{i}Pr−PCP−Rh/$PhCHN_2$ system) close to the actual experimental system.

Search for Plausible Reaction Pathways−H−PCP−Rh/$PhCHN_2$ System. The system was initially investigated (geometry optimization) at the mPW1k/SDD level.[31] To further improve the accuracy of the calculated profile, single-point-energies at this level of reference geometry were calculated at the mPW1k/SDB-cc-pVDZ level. Finally, in the preferred

(30) Dapprich, S.; Komaromi, I.; Byun, K. S.; Morokuma, K.; Frisch, M. J. *J. Mol. Struct. (THEOCHEM)* **1999**, *461*, 1 and references therein.

Scheme 5

Pathway I. Intramolecular "bound diazo" mechanism

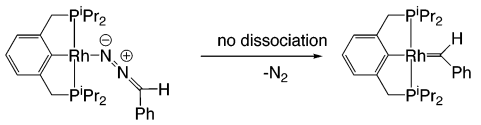

Pathway II. Intermolecular dissociative "direct attack" mechanism

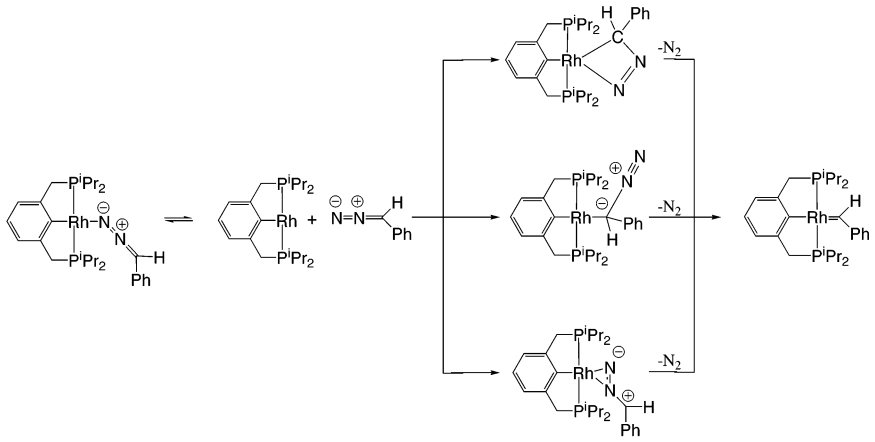

Pathway III. Bimolecular mechanism

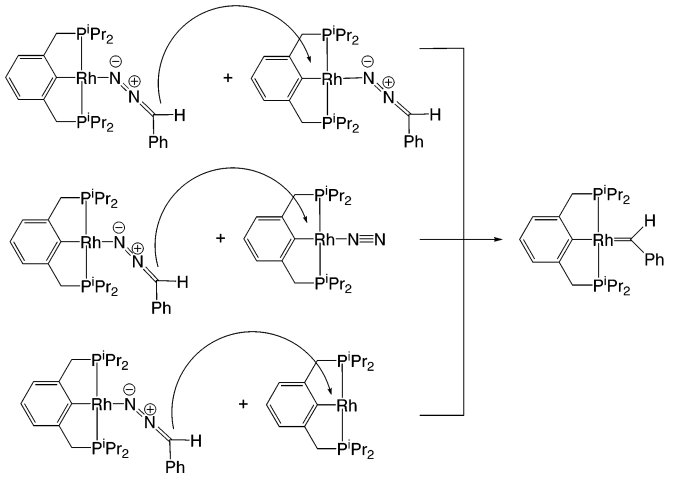

reaction profiles all the stationary points were optimized at the mPW1k/SDB-cc-pVDZ level for consistency. All of the energies reported are relative to the starting complex **1H** (Scheme 7) unless indicated otherwise. A summary of the computational results is given in Table 1.

On the basis of the relative free energy, the diazo coordination (**1H**→**3H**) can take place both by associative and dissociative mechanisms, the latter being preferable at room temperature (vide infra). the observed formation of η^1-N diazo complex **4** prior to the carbene formation (see Scheme 3) may suggest that the diazo into carbene transformation does not involve detachment of the diazoalkane throughout the carbene formation sequence (bound diazo mechanism, pathway I in Scheme 5). Thus, both "bound diazo" and "direct attack" mechanisms were explored computationally, and the following pathways were found (see Scheme 7). Following the formation of the η^1-N diazo complex **2H** from **1H**, the reaction sequence proceeds by η^1-N into η^2-NN transformation (**3H**→**4H**) with a kinetic barrier of 13.4 kcal/mol. Then there are two alternative pathways for formation of the carbene complex, while keeping the diazo molecule bound to the metal center. In the first one, the diazirine intermediate **5H** is formed and converted into an intermediate **6H** with a chelating four-membered ring (η^2-(CN)), which in turn yields η^1-C intermediate **7H** (Figure 2). An additional pathway is represented by a cleavage of a C−N bond in the four-membered ring of **6H** to give carbene nitrogen complex **8H** that loses N_2 to form the carbene complex **9H**. The latter path is kinetically more favorable. Thus, the barrier for breaking the N−C bond in **6H** to form **8H** is 4.4 kcal/mol**.** Furthermore, N_2 loss from **8H** to form the carbene complex **9H** appears to

(31) Except of the geometry of the intermediate **7H**, which was optimized at the mPW1k/SDB-cc-pVDZ level since no such stationary point was found at the mPW1k/SDD level. Instead, only intermediate **7Hi**, which is a η^2-CN complex, was found at this level (Table 1). This could be justified by the fact that complexes (**7H** and **7Hi**) have comparable energies, and they are closely related geometrically, thus only one of them was located in a given basis set. In the larger basis set (SDB-cc-pVDZ), however, only **7H** was located. This result supports the initial belief that **7H** is the intermediate involved in the mechanism.

Scheme 6

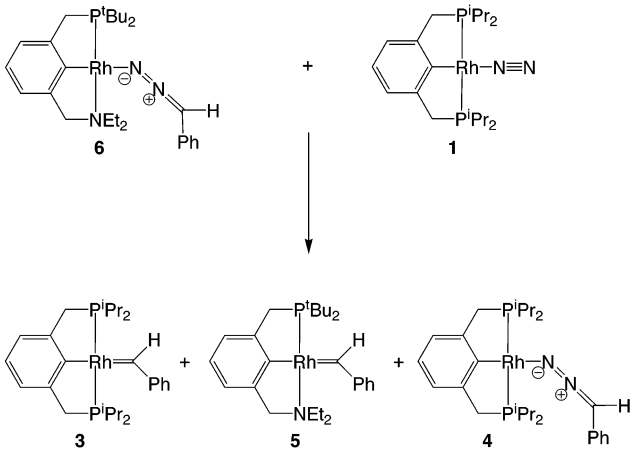

Scheme 7

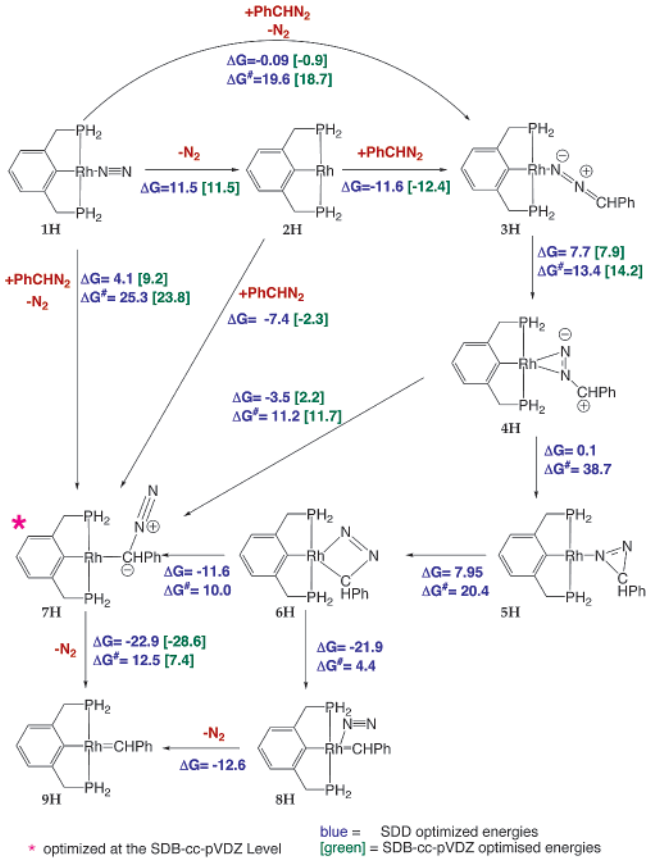

be barrierless as evident from the fact that although TS for **8H**→**9H** was located, it has a lower energy on the ΔE_e surface than of **8H** (see Table 1). The high barrier for the conversion of η^2-NN diazo complex **4H** into three-membered diazirine complex **5H** (38.7 kcal/mol) suggests that this pathway is not operative under the actual reaction conditions. It should be noted that a high barrier for the conversion of η^2-NN complex **4H** to diazirine complex **5H** is obtained even though both complexes have a similar relative energy, suggesting that this kinetic effect is due to a large amount of energy needed for the induction of strain during the formation of the diazirine. No TS for the direct **3H** or **4H** into **6H** conversion was found. It should be noted that four-membered ring η^2-(CN) diazoalkane complexes of the type **6H** were suggested to be reactive intermediates in the course of carbene formation from diazo compounds.[3]

Table 1. Relative Energies (ΔEe) and Free Energies (ΔG298) of the Various Complexes of the H−PCP and ^{i}Pr−PCP Systems (kcal/mol)

complex	ΔE_e	ΔG_{298}
H−PCP System (mPWlk/SDB-cc-pVDZ//mPWlk/SDD)		
(H−PCP)RhN2 (**1H**)	0.0	0.0
(H−PCP)Rh (**2H**)	23.1	11.5
(H−PCP)Rh−N═N═CHPh (**3H**)	0.0	−0.1
TS−Phdiazo-to-Eta2 **TS(3H-4H)**	12.8	13.3
(H−PCP)PhDiazo-NN-eta2 (**4H**)	5.9	7.6
TS−PhDiazoEta2 to Diazirine **TS(4H-5H)**	47.2	46.3
TS-eta2NNtoEtalCdiazo **TS(4H-7H)**	20.6	18.8
(H−PCP)Rh-Diazirine (**5H**)	6.2	7.7
TS-Diazirine to 4memRing **TS(5H-6H)**	26.7	28.0
(H−PCP)Rh-4memRing (**6H**)	13.6	15.6
TS-4memRing to eta1C **TS(6H-7H)**	25.6	25.6
TS-4memRing to CarbeneN2 **TS(6H-8H)**	19.3	20.0
(H−PCP)Rh- -CHPh═N═N[a] (**7H**)	6.1[a]	4.0[a]
(H−PCP)PhDiazo-CN-eta2 (**7Hi**)	10.8	12.4
TS-DiazCarbon-to-Carbene **TS(7H-9H)**	17.6	16.5
(H−PCP)PhCarbeneN2 (**8H**)	−6.3	−6.3
TS−CarbeneN2 to Carbene **TS(8H-9H)**	−7.1	−10.2
(H−PCP)PhCarbene (**9H**)	−6.9	−18.8
TS−RhN2toRhDiazoEtal **TS(1H-3H)**	11.1	19.7
TS−RhN2toRhEtalC **TS(1H-7H)**	15.6	25.3
(H−PCP)Rh-Diazo-Rh (**10H**)	−14.3	−0.6
H−PCP Svstem (mPWlk/SDB-cc-pVDZ)		
(H−PCP)RhN2 (**1H**)	0.0	0.0
(H−PCP)Rh (**2H**)	23.0	11.5
(H−PCP)Rh−N═N═CHPh (**3H**)	0.2	−0.9
TS−Phdiazo-to-Eta2 **TS(3H-4H)**	12.6	13.3
(H−PCP)PhDiazo-NN-eta2 (**4H**)	5.5	7.0
TS-eta2NNtoEtalCdiazo **TS(4H-7H)**	20.3	18.7
(H−PCP)Rh- -CHPh═N═N (**7H**)	9.2	9.2
(H−PCP)Rh- -(CH)Ph═N═N Agostic (**7Hii**)	8.7	8.8
TS-DiazCarbon-to-Carbene **TS(7H-9H)**	17.5	16.6
(H−PCP)PhCarbene (**9H**)	−7.3	−19.4
TS−RhN2toRhDiazoEtal **TS(1H-3H)**	10.3	18.7
TS−RhN2toRhEtalC **TS(1H-7H)**	14.8	23.8
^{i}Pr−PCP System (mPWlk/LANL2DZ+P//ONIOM(mPWlk/LANL2DZ: mPWlk/LANLlMB)		
(^{i}PrPCP)RhN2 (**1P**)	0.0	0.0
(^{i}Pr−PCP)Rh (**2P**)	27.5	15.8
(^{i}Pr−PCP)Rh−N═N═CHPh (**3P**)	1.4	2.0
TS-^{i}Pr−Phdiazo-to-Eta2 **TS(3P-4P)**	15.0	16.6
^{i}Pr−PhDiazo-NN-eta2 (**4P**)	12.1	15.7
TS-^{i}Pr-eta2NNtoFreeDiazo **TS(4P-2P)**	23.9	24.0
TS-^{i}Pr-eta2NN-Diazirine **TS(4P-5P)**	49.0	49.9
(^{i}Pr−PCP)Rh-Diazirine (**5P**)	8.9	11.2
(^{i}Pr−PCP)Rh-4memRing (**6P**)	20.3	24.9
(^{i}Pr−PCP)Rh- -CHPh═N═N (**7P**)	17.4	18.1
^{i}Pr−PhDiazo-CN-eta2 (**7Pi**)	17.8	21.9
TS-^{i}Pr-DiazCarbon-to-Carbene **TS(7P-9P)**	27.9	29.1
(^{i}Pr−PCP)PhCarbene-perpendicular (**9P$_{ppd}$**)	5.2	−5.6
(^{i}Pr−PCP)PhCarbene-parallel (**9P$_{prl}$**)	4.8	−5.9
(^{i}Pr−PCP)Rh-Diazo-Rh (**l0P**)[b]	−2.7	15.8
(^{i}Pr−PCP)Rh-Dimer (**11P**)	4.4	8.6

[a] Optimized in SDB-cc-pVDZ basis set. [b] With respect to 3P+2P.

The second possible pathway in the "bound diazo" mechanism involves η^2-NN to η^1-C transformation (**4H**→**7H**) with subsequent N_2 loss (Scheme 7, Figure 3). The barrier for η^1-N into η^2-NN is 13.4 kcal/mol, and η^2-NN in η^1-C is 11.2 kcal/mol, values which are reasonable for this mechanism operating in H−PCP system at room temperature and below.

Analysis of the temperature dependence of the ΔG surface reveals that at room temperature the dissociative path (**1H** → **2H** → **3H**) is more likely to take place (11.5 kcal/mol for dissociative vs 19.7 kcal/mol for associative path) and at low

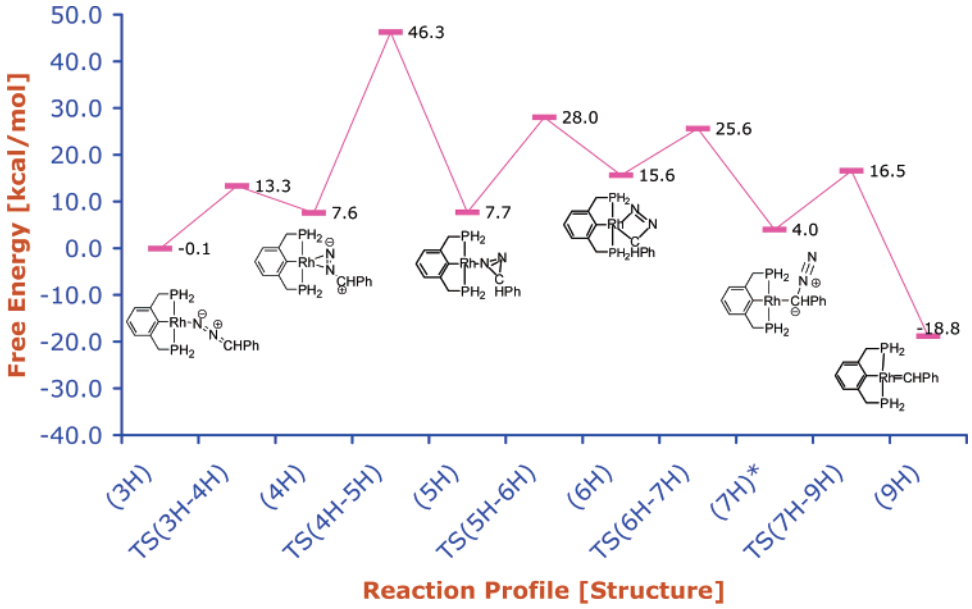

Figure 2. H-PCP system, bound mechanism-diazirine pathway, reaction profile (ΔG_{298}) at mPW1k/SDB-cc-pVDZ//mPW1k/SDD Level.

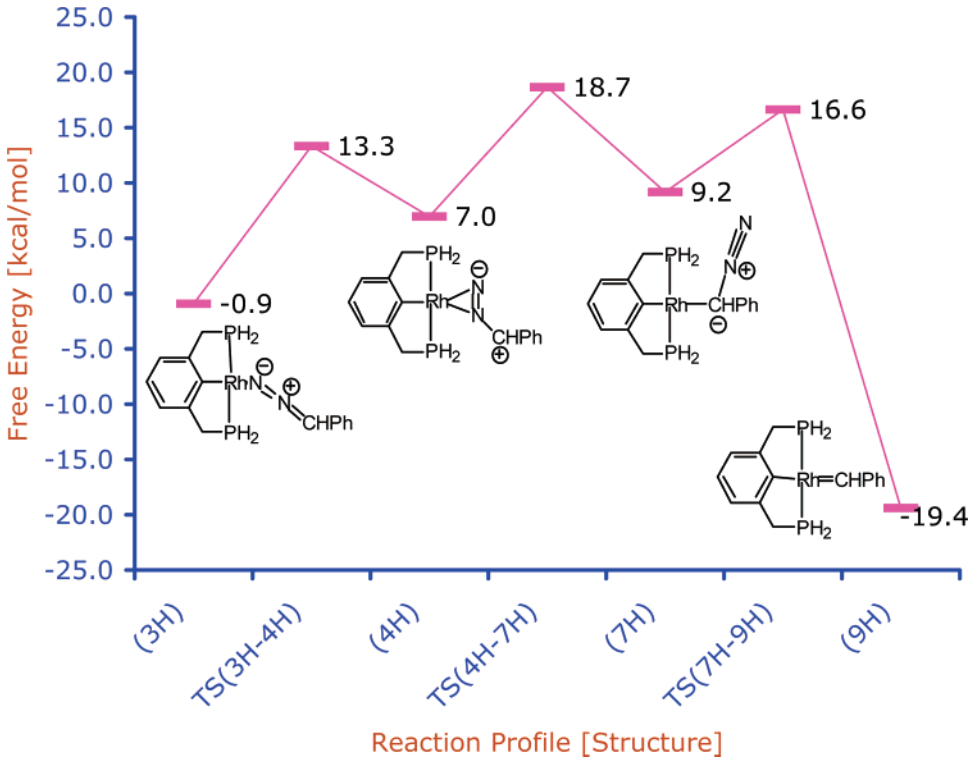

Figure 3. H-PCP system, bound mechanism-η^2-NN pathway, reaction profile (ΔG_{298}) at mPW1k/SDB-cc-pVDZ Level.

temperature (i.e., −70 °C) the dissociative and associative (**1H** → **3H**) paths are energetically fairly comparable (14.8 vs 16.7 kcal/mol). Already in the H−PCP system, however, the associative reaction to form **7H** via direct reaction of **1H** with $PhCHN_2$, has a relatively high barrier both at low and room temperatures (22.0 and 25.3 kcal/mol, respectively).

A direct attack of the $PhCHN_2$ carbon atom on the metal center of intermediate **2H** (or **1H**) to form **7H** (pathway II, Scheme 5) is definitely a plausible alternative to the "bound diazo" scheme.

Because optimization of **7H** was carried out in a larger basis set (SDB-cc-pVDZ), all the intermediates involved in the "direct attack" pathway and transition states were also optimized at this level of theory for the sake of consistency (Scheme 7, Table 1, Figure 3). Optimization of all structures presented in Scheme 7 in this basis set was beyond our computational resources and appears redundant due to the intrinsically high energy of the diazirine pathway. It can be noticed that the net effect of using the larger basis set is destabilization of **7H** with respect to its relative energy in the smaller basis set calculations. Thus, for

example, **7H** is only slightly more stable (by 2.3kcal/mol) than the Rh-T shape intermediate **2H**. The feasibility of N_2 dissociation from **1H** and $PhCHN_2$ coordination through the carbon atom implies that there is a possibility of direct η^1-C diazoalkane binding to the metal center, the mode favorable for carbene formation.

An additional pathway (pathway III, Scheme 5) leading to carbene formation is represented by a bimolecular route. A complete search for such a mechanism was beyond our computational resources, but intermediate **10H** (see Table 1), which is a two-metal center complex containing one diazo molecule, could be located. This intermediate, in which one Rh center is coordinated to the carbon atom and the second Rh is coordinated to the terminal nitrogen, could lead to the formation of the carbene (together with a formation of the Rh−N_2 starting material, **1H**) by N−C cleavage, since the carbon atom of the diazo molecule is already activated by the second Rh-center. Moreover, it seems to be comparable in energy (see Table 1) to the two individual intermediates (**3H** and **2H**) in the H−PCP system.

In short, our computational results for the **H−PCP−Rh/$PhCHN_2$** system can be summarized as follows. Formation of carbene complex in a system *with H-substituents on the phosphine arms* may proceed by two conceptually different mechanisms, both leading to the η^1-C intermediate **7H**: (1) a "bound diazo" mechanism in which the $PhCHN_2$ molecule stays bound to the metal center throughout the whole reaction; (2) a "direct attack" pathway in which the η^1-N complex **3H** is a resting state. Bimolecular mechanism cannot be ruled out for the H−PCP system. However, in principle, it is very similar to the 'direct attack' mechanism, as both of them require the prior coordination of the Rh center to the carbon atom of the $PhCHN_2$ as a key step leading the formation of the carbene. To verify these findings and to investigate the feasibility of other mechanisms, we introduced ^{i}Pr substituents in an ONIOM method in order to analyze the system having the closest similarity to the experimental one.

^{i}Pr−PCP−Rh/$PhCHN_2$ System (ONIOM). Suggested Reaction Pathway. Geometry optimizations were performed at the ONIOM(mPW1k/LANL2DZ:mPW1k/LANL1MB) level, starting from the previously optimized mPW1k/LANL2DZ geometries for the H−PCP inner layer. The outer layer (mPW1k/LANL1MB) included only the ^{i}Pr substituents on the phosphine arms. To improve the reliability of the results, all-atom single point energies calculations at the mPW1k/LANL2DZ+P level were performed at the optimized geometries. The results of the calculations are presented in Scheme 8, Figure 4, and Table 1. First, we considered direct attack of the phenyl diazomethane on the metal center. Both dissociative (through T-shaped intermediate **2P**) and associative (through dinitrogen complex **1P**) mechanisms were tested but no transition states could be found for the associative mechanisms. It is conceivable that the associative attack of $PhCHN_2$ on ^{i}PrPCP−Rh−N_2 complex **1P** will be unfavorable in comparison to dissociative loss of N_2 due to the steric interference imposed by the bulky ^{i}Pr substituents. Because already for the H−PCP system the barrier for the associative attack was relatively high (23.8 kcal/mol for the carbon attack and 18.7 kcal/mol for nitrogen attack) to take place at low temperatures, it is expected that this barrier will increase with increasing steric bulk. It was shown experimentally

Scheme 8

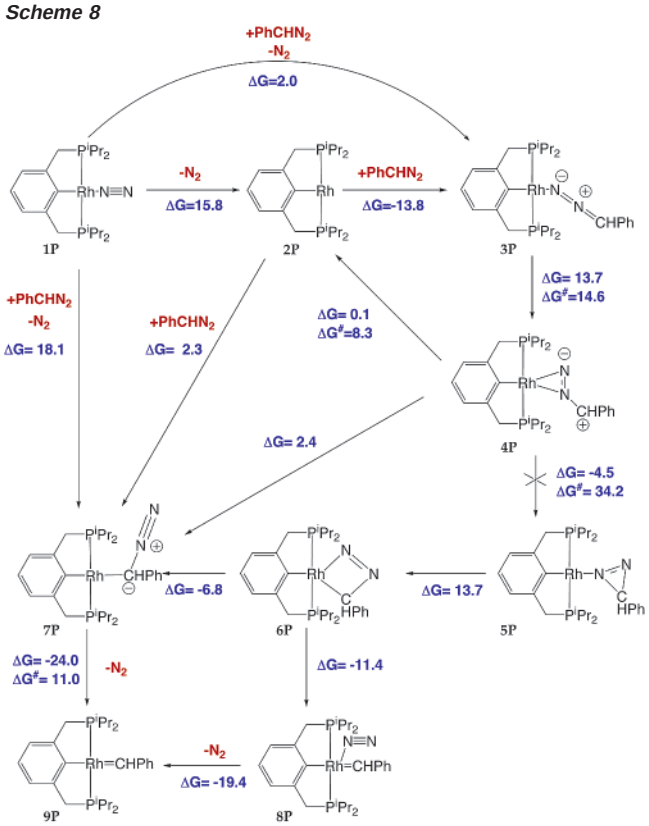

that complexes $HRhL_2(N_2)$ (L = P^tBu_3, P^iPr_3, PCy_3) release nitrogen to form three-coordinate $HRhL_2$ species in the case of P^tBu_3 and PCy_3, and dimer dinitrogen complex $HL_2Rh(N_2)$-$RhHL_2$ (similar to **1b**) in the case of P^iPr_3.[26] Thus, dissociative N_2 loss most probably also takes place in our system, which is electronically and sterically very similar to the above-mentioned ones. The Rh dinitrogen complex dimer−monomer equilibrium (Scheme 9) is also a feasible process to produce the T-shaped compound **2P**. The possible modes of the phenyl diazomethane bonding are η^1-N, η^2-NN, η^1-C, η^2-CN, and η^2-(CN) (four-membered ring). Although η^1-N bonding is degenerate, the cyclic η^2-(CN) complex **6P** is higher in energy by ~9 kcal/mol than the η^1-N diazo complex; thus, is not expected to be formed. (Furthermore, a TS for the coordination of free $PhCHN_2$ to Rh-T shaped in a η^2-(CN) bonding mode, was located and found to be ~25 kcal/mol higher in energy than the Rh-T shape intermediate). Only η^2-NN, η^2-CN and η^1-C modes were found to be viable. The η^2-CN complex (**7Pi**) is closely related to **7P** both geometrically and energetically (Table 1). Although no TS(**7P**→**7Pi**) was found, it is expected that the interconversion between these two complexes is relatively low in energy. It should be noted that for the H−PCP system, only the η^2-CN complex (**7Hi**) was found in the small SDD basis set, however in the larger SDB-cc-pVDZ basis set, only **7H** was found, indicative of the large resemblance between these two complexes already in the H−PCP model system.

It appears that the coordination of phenyl diazomethane through the carbon atom, although less favorable than in the H−PCP case (probably due to the steric bulk), is an energetically plausible process leading to the carbene complex. Our attempts to find a TS connecting **4P**, the η^2-NN complex, and **7P**, the η^1-C complex (TS similar to the one found for the H−PCP system), invariably lead to detachment of the phenyl diazo-

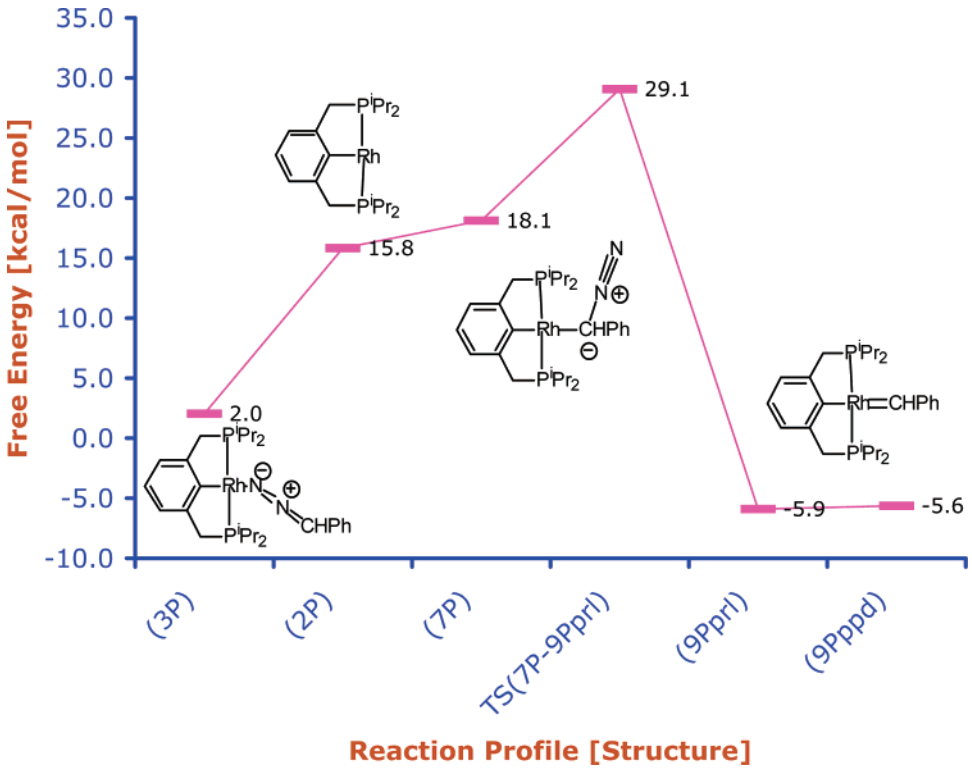

Figure 4. ^{i}Pr−PCP system, Detached Mechanism pathway, reaction profile (ΔG_{298}) at mPW1k/LANL2DZ+P//ONIOM(mPW1k/LANL2DZ:mPW1k/LANL1mb) Level.

Scheme 9

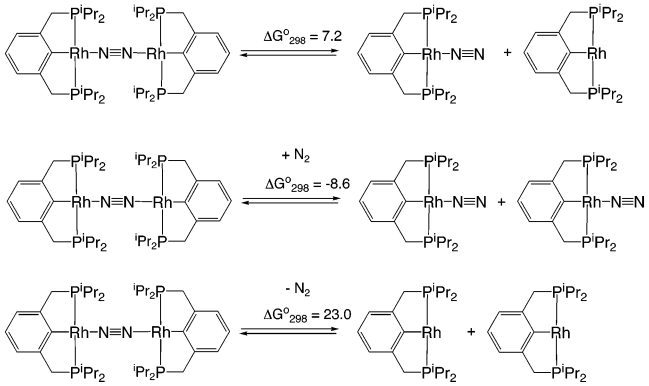

methane. Thus, TS for the transformation of **7P** (η^2-NN) to Rh-T shaped complex **2P** and free $PhCHN_2$ was found (Table 1). This process has a barrier of 8.3 kcal/mol, suggesting that when the η^2-NN complex is formed, there is a low barrier for dissociation of the diazo molecule.[32] We believe that in the real system a TS for **4P→7P** transformation most probably is not accessible due to a steric effect hindering the approach of the carbon atom from an η^2-NN conformation of the diazo. Further support for this assumption may be obtained by examining the geometry of the TS(**4H→7H**) found for the H−PCP system (Figure 5).

In this TS, the phenyl ring is situated in close proximity to the phosphine arm, such that the phenyl group is expected to interfere with the ^{i}Pr substituents in the case of the ^{i}Pr−PCP system. We believe that in the "direct attack" scheme the free $PhCHN_2$ is less geometrically restricted to form an η^1-C

(32) TS's are normally difficult to find for association and dissociation of ligands since it mostly involves entropic contribution, which cannot be calculated on the bottom-of-the-well energy surface. Here, it was found probably due to the relatively large geometrical change in the diazo molecule when coordinated to the metal.

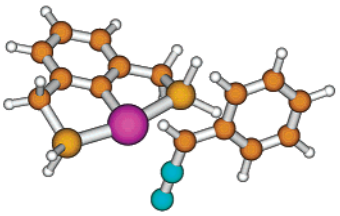

Figure 5. **TS(4H-7H)** transition state between η^2-NN to η^1-C diazo complexes of H−PCP system.

intermediate. Due to the apparently low barrier of the diazo dissociation and energetic availability of η^1-C intermediate **7P** the "direct attack" mechanism appears to operate in the ^{i}Pr−PCP−Rh/$PhCHN_2$ system. The "bound diazo" mechanism seems to be the less probable situation, although we cannot completely rule out its operating concurrently with the "direct attack" mechanism. The pathway proceeding through diazirine intermediate is intrinsically high in energy also for the ^{i}Pr−PCP system, as can be observed from the high barrier for the formation of the diazirine complex, **TS(4P-5P)** (Scheme 8, Table 1).

As far as the bimolecular mechanism (pathway III, Scheme 5) is concerned, the complete search for such a mechanism was beyond our computational resources. We were able to locate the intermediate **10P**, (see Figure 6) with two PCP−Rh moieties coordinated to the nitrogen and carbon of the phenyl diazomethane. It is about 16 kcal/mol higher in energy than **2P**+**3P**. Formation of **10P** is likely to be preceded by the formation of **2P**, and thus, the formation of **7P** from **2P** and free diazoalkane seems to be energetically preferable (ΔG = 2.3 kcal/mol, Scheme 8), favoring the direct attack pathway. It should be noted that our experimental observations suggest the bimolecular pathway to be less probable than the direct attack one. Thus,

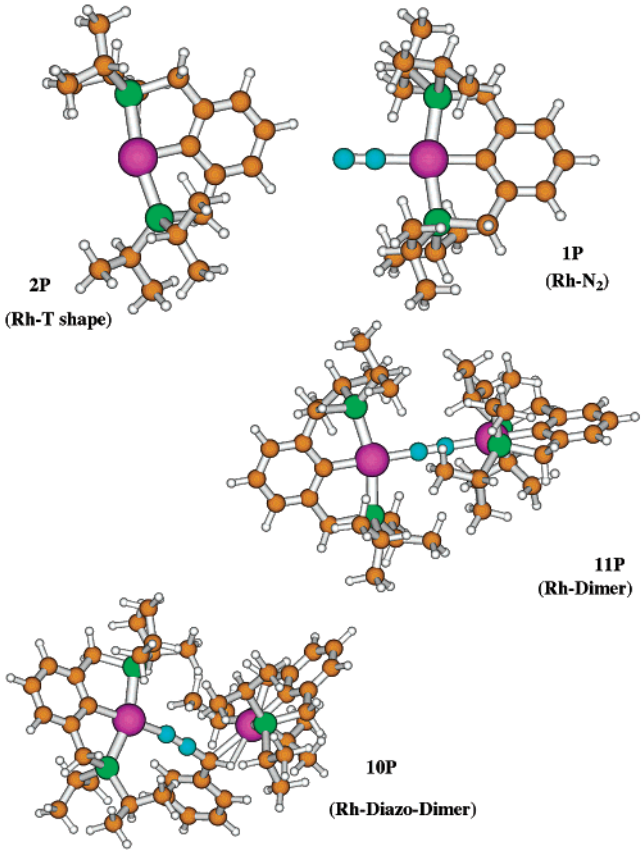

Figure 6. 3D structures of **1P**, **2P**, **10P**, and **11P**.

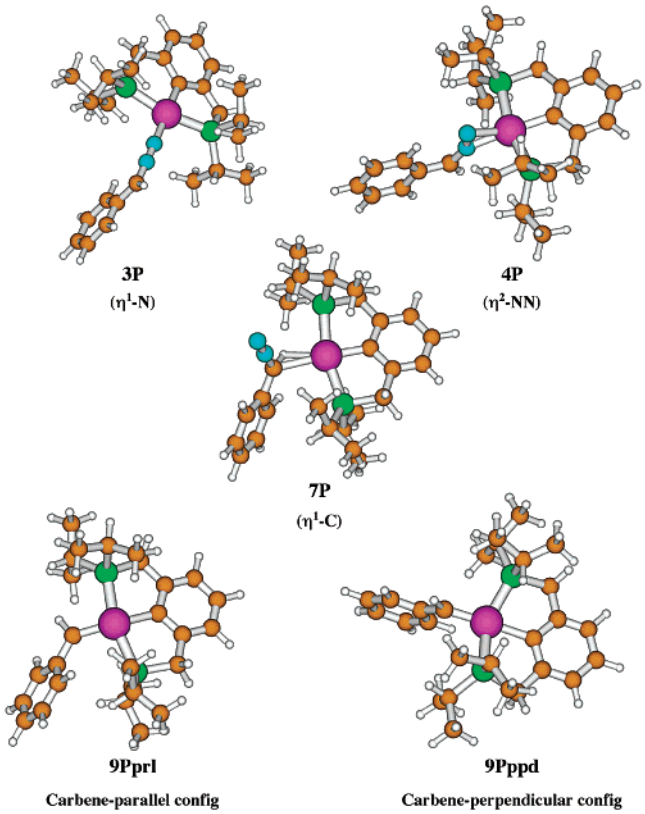

Figure 7. 3D structures of intermediates **3P**, **4P**, **7P**, $\mathbf{9P_{prl}}$, and $\mathbf{9P_{ppd}}$.

we can tentatively rule out the bimolecular pathway III (Scheme 5). In any case, in the bimetallic intermediate **10P**, the key interaction leading to a carbene complex is η^1-C coordination of phenyldiazomethane.

Thus, the direct coordination of the diazo compound through the carbon atom, followed by the loss of N_2, appears to be the most plausible reaction pathway. On the basis of the experimental and computational studies the following arguments favor this conclusion. (1) The metallacarbene formation takes place at a temperature at which the diazoalkane is starting to decoordinate from the metal center. (2) If the "bound diazo" scheme were operating starting from the observed η^1-N diazo complex, no side reactions ought to take place in the course of the metallacarbene formation, contrary to our experimental observations. (3) The low computed barrier for η^1-N $-$ η^2-NN transformation and the low barrier of subsequent $PhCHN_2$ dissociation suggest that the "direct attack" scheme is favored. (4) Other pathways were computed to be intrinsically high in energy. (5) Formation of η^1-C complex **7P** is energetically feasible. (6) Complex **7P** is a key intermediate (one step before the carbene formation), *in almost all of the computed reaction pathways*.

Structure of the Key Compounds. The calculated structures of **1P**, **2P**, **10P**, **11P (dimer)**, **3P**, **4P**, **7P**, $\mathbf{9P_{prl}}$, and $\mathbf{9P_{ppd}}$ are presented in Figures 6 and 7. The bond lengths and bond orders (Wiberg NBO analysis) are given in Table 2.

The dinitrogen complex **1P** has the square planar geometry expected for $16e^-$ Rh(I) complexes. The N_2 molecule is coordinated in an end-on mode and the N−N bond length is close to the free N_2, so it is not activated. The geometry of the η^1-N diazoalkane complex **3P** is also square planar, with the general structure of the PCP−Rh core being almost identical to that of **1P**, reflecting very similar coordination behavior, e.g., trans-influence, of N_2 and $PhCHN_2$. The NN*C* axis in **3P** is linear, the coordinated $PhCHN_2$ being very close in geometry to a free $PhCHN_2$. In η^2-NN complex **4P** the NN bond is lengthened in comparison to **3P** and free $PhCHN_2$ (bond order 1.70 vs 2.06) as expected for side-on NN coordination. The η^1-C complex **7P** has a weak Rh−C bond as evident from the corresponding bond order (0.1) and length (2.45 Å). It should be noted that ONIOM geometry optimization at the aforementioned computational level for this complex lead only to the closely related C−H agostic form where as in the H−PCP system, two distinct stationary points were found for the η^1-C and C−H agostic geometries (**7H** and **7Hii**, respectively). In the H−PCP system the two complexes differed in their relative energy only in about 0.4 kcal/mol (see Table 1) and the TS for conversion between them is expected to be very low. Thus, it could be that the small energy difference together with small geometry change lead to a flat energy surface in which only one geometry could be located in the case of ONIOM calculation. The complex can be viewed as an agostic one due to the relatively short Rh−H distance (2.03 Å), although the diazo C−H bond is not lengthened substantially in comparison to the one in complexes **3P**, **4P** and free $PhCHN_2$.

Carbene Unit Rotation. Although for the H−PCP system only one optimized geometry was found for the carbene complex **9H**, for the ^{i}Pr−PCP system we found two stationary points for the carbene complex, $\mathbf{9P_{prl}}$ and $\mathbf{9P_{ppd}}$ (Figure 7), both structures being nearly isoenergetic. this is also reflected in very similar bond lengths and bond order values (see Figure 4, Table 2) Complex $\mathbf{9P_{prl}}$ adopts a parallel configuration of the carbene unit to the PCP surface and $\mathbf{9P_{ppd}}$ a perpendicular one. The

Table 2. Bond Angles (deg) and Lengths (Å) as Well as Bond Orders of Selected Complexes of the ^{i}Pr−PCP System at ONIOM(mPWlk/LANL2DZ:mPWlk/LANL1MB) Level of Theory

	free PhCHN2		3P		4P		7P		9Pprl		9Pppd	
bond angles	N−N−C_{diazo}	179.2	P−Rh−P	164.4	P−Rh−P	162.7	P−Rh−P	163.9	P−Rh−P	164.4	P−Rh−P	148.6
	N−C_{diazo}−C_{Ph}	122	C_{ipso}−Rh−N	177.4	N−N−C_{diazo}	144.7	C_{ipso}−Rh−C_{diazo}	174.3	C_{ipso}Rh−$C_{carbene}$	154.7	C_{ipso}−Rh−$C_{carbene}$	176.2
	N−C_{diazo}-H	116.3	Rh−N−N	177.4	N−C_{diazo}−C_{Ph}	122.5	N−N−C_{diazo}	178.8	Rh−$C_{carbene}$−C_{Ph}	134.3	Rh−$C_{carbene}$−C_{Ph}	128.6
			N−N−C_{diazo}	175.5								
bond lengths	N−N	1.16	Rh−P	2.33	Rh−P	2.34	Rh−P	2.34	Rh−P	2.33	Rh−P	2.32
	N−C_{diazo}	1.3	C_{ipso}−Rh	2.05	C_{ipso}−Rh	2.05	C_{ipso}−Rh	2.02	C_{ipso}−Rh	2.1	C_{ipso}−Rh	2.15
	C_{diazo}−C_{Ph}	1.45	Rh−N	1.95	Rh−$N_{terminal}$	2.13	Rh−C_{diazo}	2.45	Rh−$C_{carbene}$	1.91	Rh−$C_{carbene}$	1.91
	C_{diazo}−H	1.08	N−N	1.17	Rh−$N_{internal}$	2.07	Rh−H_{diazo}	2.03	$C_{carbene}$−C_{Ph}	1.48	$C_{carbene}$−C_{Ph}	1.47
			N−C_{diazo}	1.3	N−N	1.24	N−N	1.15	$C_{carbene}$−H	1.1	$C_{carbene}$−H	1.1
			C_{diazo}−C_{Ph}	1.45	N−C_{diazo}	1.31	N−C_{diazo}	1.31				
			C_{diazo}−H	1.08	C_{diazo}−C_{Ph}	1.45	C_{diazo}−C_{Ph}	1.46				
					C_{diazo}−H	1.07	C_{diazo}−H	1.1				
bond orders	N−N	2.29	Rh−P	0.43	Rh−P	0.41	C_{ipso}−Rh	0.69	Rh−P	0.41	Rh−P	0.44
	N−C_{diazo}	1.4	C_{ipso}−Rh	0.57	C_{ipso}−Rh	0.58	Rh−C_{diazo}	0.1	C_{ipso}−Rh	0.42	C_{ipso}−Rh	0.39
	C_{diazo}−C_{Ph}	1.1	Rh−N	0.55	Rh−$N_{terminal}$	0.62	Rh−H_{diazo}	0.05	Rh−$C_{carbene}$	1.09	Rh−$C_{carbene}$	0.92
			N−N	2.06	Rh−$N_{internal}$	0.33	N−N	2.32	$C_{carbene}$−C_{Ph}	1.11	$C_{carbene}$−C_{Ph}	1.15
			N−C_{diazo}	1.38	N−N	1.7	N−C_{diazo}	1.34				
			C_{diazo}−C_{Ph}	1.11	N−C_{diazo}	1.4	C_{diazo}−C_{Ph}	1.08				
					C_{diazo}−C_{Ph}	1.13						

parallel geometry is most probably electronically more favorable (larger Rh═C bond order is observed for the parallel carbene **9P$_{prl}$**: 1.09 in **9P$_{prl}$** vs 0.92 in **9P$_{ppd}$**), whereas the perpendicular one is sterically preferred. We believe that the barrier for the interconversion between the two conformations is low, although no TS was located. Experimentally, the symmetric NMR pattern of the carbene complex suggests that the rotation of the carbene unit takes place and it is a very facile process. It is further supported by the observation of a pattern characteristic of a symmetric system even at −70 °C in the NMR spectra of **2**. It has been reported that no barrier for carbene rotation could be detected even below −100 °C, implying it must be very low.[33]

The experimental and computed structures of the Rh−^{i}PrPCP dinitrogen dimer reactant are presented in Figures 1 and 6, respectively. There is good agreement between the computed and the X-ray structures (see details in Supporting Information).

Discussion

Our experimental observations and computational studies suggest that at low temperatures reaction of the Rh(I) complex with phenyl diazomethane leads to formation of the η^1-N diazo complexes and that coordination of the diazoalkane is reversible upon warming. Binding of the diazoalkane to the metal through carbon (η^1-C) and subsequent N_2 loss result in metallacarbene formation. The formation mechanism of the putative metallacarbene in the course of the cyclopropanation reaction was studied computationally,[9c,d] concluding that it involves initial diazoalkane coordination through the carbon atom, followed by loss of N_2. However, other pathways, involving coordination through the nitrogen atoms, were not investigated. In one experimental study, an intermediate in the cyclopropanation reaction with a diazoalkane coordinated through carbon atom was observed at low temperature.[21]

It is generally recognized that formation of diazoalkane complexes coordinated through N (either by η^1-N or η^2-NN) may stabilize the diazo compounds. There are many examples of stable diazoalkane complexes demonstrating η^1-N or η^2-NN coordination modes. Generally, they do not form carbene complexes, and seem to play either competitive or spectator roles in the metallacarbene formation.

It is known that careful choice of ligands and diazo compounds is crucial in order to achieve carbene complex formation. A balance is always struck between the kinetic availability of the carbene complex and its thermodynamic stability. Thus, one of the main strategies is reacting a diazoalkane with a metal complex bearing a specific set of ligands, to be substituted by another set of more bulky ligands once the carbene complex is formed.[5,12] The choice of the diazo compounds and ligands that result in carbene complex formation, is normally very limited.

We surmise that the reactivity observed in our PCP and PCN−Rh systems and in other late transition metal systems is controlled mainly by steric factors. Because formation of the carbene complex requires prior η^1-C diazo coordination, this process is sterically demanding, far more so than η^1-N or η^2-NN coordination, as reflected in the relative stability of these compounds. Thus, an important requirement for the carbene formation is the viability of an η^1-C coordinated diazo complex. The process could not be facilitated by formation of an η^1-N coordinated diazo complex; on the contrary, its formation seems to interfere in many cases with carbene formation. It has been suggested that a cyclic η^2-(CN) intermediate containing a four-membered ring is an intermediate in the course of carbene synthesis.[3] Our study shows that in the case of bulky substituents this mechanism as well as mechanisms proceeding through an η^2-NN intermediate ("bound diazo" scheme) are unlikely to be operative. On the other hand, in the less bulky H−PCP ligand system both "bound diazo" and "direct attack" pathways can take place.

The importance of steric factors in the formation of the critical η^1-C bound diazo complex intermediate seems to be paramount. Thus, adding ^{i}Pr substituents in our DFT study diminished the stability of the η^1-C intermediate **7P** due to steric repulsion. Additional evidence for the importance of steric factors is best demonstrated in the work of Werner et al.[5,14] (Scheme 10). In their approach, a Rh complex bearing Sb^{i}Pr$_3$ ligands is reacted with Ph_2N_2 to produce a metallacarbene. Stibane ligands are then substituted by P^{i}Pr$_3$ to give a stable carbene complex. When

(33) Manganiello, F. J.; Radcliffe, M. D.; Jones, W. M. *J. Organomet. Chem.* **1982**, *228*, 273.

Scheme 10

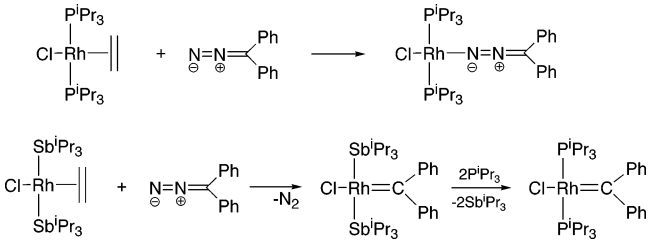

a Rh complex bearing ^{i}Pr ligands is reacted with Ph_2N_2, an η^1-N diazo complex is formed. Stibane ligands most probably serve as a less crowded analogue of phosphines due to their smaller cone angle resulting from the larger atomic radius of Sb compared to P. As a consequence, the metal center is less sterically impeded and the η^1-C diazo intermediate can be formed. The same probably holds for the Ru carbene synthesis using diazo alkanes by Grubbs et al.[12] In this synthesis, $(PPh_3)_3RuCl_2$ and phenyldiazomethane are utilized. Following the carbene formation, PCy_3 is added to produce a more stable, sterically shielded carbene. The direct synthesis starting with the precursor bearing PCy_3 ligands is most probably difficult due to steric reasons. It should be noted that generally, with a given set of ligands on a metal center, only a narrow selection of diazo alkanes can be used to produce a carbene complex. Smaller diazoalkanes normally produce unstable carbenes (that decompose by dimerization), while larger diazoalkanes give η^1-N bound diazo complexes, due to the difficulty in formation of the essential η^1-C diazo complex, which is sterically demanding. The η^1-N binding is obviously less sterically demanding and η^1-N complexes can be formed with a large variety of metal complexes. Thus, the fit between diazoalkane size and ligand bulk is a factor requiring the utmost consideration.

Regarding the electronic factors, the availability of a vacant coordination site is crucial. In almost all cases, metal precursors for carbene complexes have either a free coordination site or an ability to create one. We believe that the design of systems for the production of metallacarbenes using diazo alkanes should include a coordinatively unsaturated metal precursor and careful consideration of steric factors, i.e., diazoalkane fit to the steric crowding on the metal. Then the stability of the resulting carbene has to be considered: it can be increased with bulky ligands, protecting the carbene from dimerization and external attack by solvent or other reagents.

Conclusions

We have carried out an experimental and computational study of carbene complex formation from phenyl diazomethane in PCN and PCP−Rh systems. Our studies show that end-on η^1-N complex formation precedes the formation of the carbene complex in both cases. Coordination of $PhCHN_2$ to the metal centers in PCP and PCN systems was found to be reversible both experimentally and computationally. The diazo η^1-N complex appears to be rather a side equilibrium resting state and not an essential intermediate for carbene formation. The DFT calculations reveal that the key intermediate for the metallacarbene formation is an η^1-C diazo complex. Its formation proceeds most probably by a direct attack of the diazo molecule on the metal center. As a consequence, steric factors play an important role in the carbene complex formation from diazoalkanes. Design of systems for formation of transition metal carbenes from diazoalkanes should involve a coordinatively unsaturated metal precursor and careful consideration of steric factors, i.e., a proper diazoalkane fitting to the steric requirements of the metal center.

Computational Methods

All of the calculations were carried out using the Gaussian 98 program revisions A.7[34] and A.11[35] running on Compaq ES40 and XP1000 workstations as well as on a mini-farm of Pentium IV Xeon 1.7/2.0 GHz PC's running Red Hat Linux 7.2 in our group, on an experimental Linux PC Farm at the Faculty of Physics, and on the (Israel) Inter-University Computing Center (IUCC) SGI Origin 2000. (The patch to *Gaussian 98* rev A.7 as detailed in the Appendix to ref 36 was applied.)

For the H−PCP system the mPW1k (modified Perdew-Wang 1-parameter for kinetics) exchange-correlation functional of Truhlar and co-workers[37] was employed in conjunction with the SDD and SDB-cc-pVDZ basis sets (see below). The mPW1k functional was very recently shown[37,38] to yield more reliable reaction barrier heights than other exchange-correlation functionals.

The SDD basis set is the combination of the Huzinaga−Dunning double-ζ basis set on lighter elements with the Stuttgart−Dresden basis set−relativistic effective core potential (RECP) combination[39] on the transition metals. The SDB-cc-pVDZ basis set, combines the Dunning cc-pVDZ basis set[40] on the main group elements with the Stuttgart−Dresden basis set-RECP combination[39] on the transition metals, with an *f*-type polarization exponent taken as the geometric average of the two *f*-exponents given in the Appendix to ref 41.

For the ^{i}Pr−PCP, as in our previous studies on the PCP,[42] PCN,[43] and PCO[44] systems, the initial survey of the potential surface was carried

(34) Frisch, M. J.; Trucks, G. W.; Schlegel, H. B.; Scuseria, G. E.; Robb, M. A.; Cheeseman, J. R.; Zakrzewski, V. G.; Montgomery, J. A.; Stratmann, R. E.; Burant, J. C.; Dapprich, S.; Millam, J. M.; Daniels, A. D.; Kudin, K. N.; Strain, M. C.; Farkas, O.; Tomasi, J.; Barone, V.; Cossi, M.; Cammi, R.; Mennucci, B.; Pomelli, C.; Adamo, C.; Clifford, S.; Ochterski, J.; Petersson, G. A.; Ayala, P. Y.; Cui, Q.; Morokuma, K.; Malick, D. K.; Rabuck, A. D.; Raghavachari, K.; Foresman, J. B.; Cioslowski, J.; Ortiz, J. V.; Stefanov, B. B.; Liu, G.; Liashenko, A.; Piskorz, P.; Komaromi, I.; Gomperts, R.; Martin, R. L.; Fox, D. J.; Keith, T.; Al-Laham, M. A.; Peng, C. Y.; Nanayakkara, A.; Gonzalez, C.; Challacombe, M.; Gill, P. M. W.; Johnson, B. G.; Chen, W.; Wong, M. W.; Andres, J. L.; Head-Gordon, M.; Replogle, E. S.; Pople, J. A.; *Gaussian 98*, Revision A.7; Gaussian, Inc.: Pittsburgh, PA, 1998.

(35) Frisch, M. J.; Trucks, G. W.; Schlegel, H. B.; Scuseria, G. E.; Robb, M. A.; Cheeseman, J. R.; Zakrzewski, V. G.; Montgomery, J. A. Jr.; Stratmann, R. E.; Burant, J. C.; Dapprich, S.; Millam, J. M.; Daniels, A. D.; Kudin, K. N.; Strain, M. C.; Farkas, O.; Tomasi, J.; Barone, V.; Cossi, M.; Cammi, R.; Mennucci, B.; Pomelli, C.; Adamo, C.; Clifford, S.; Ochterski, J.; Petersson, G. A.; Ayala, P. Y.; Cui, Q.; Morokuma, K.; Salvador, P.; Dannenberg, J. J.; Malick, D. K.; Rabuck, A. D.; Raghavachari, K.; Foresman, J. B.; Cioslowski, J.; Ortiz, J. V.; Baboul, A. G.; Stefanov, B. B.; Liu, G.; Liashenko, A.; Piskorz, P.; Komaromi, I.; Gomperts, R.; Martin, R. L.; Fox, D. J.; Keith, T.; Al-Laham, M. A.; Peng, C. Y.; Nanayakkara, A.; Challacombe, M.; Gill, P. M. W.; Johnson, B.; Chen, W.; Wong, M. W.; Andres, J. L.; Gonzalez, C.; Head-Gordon, M.; Replogle, E. S. and Pople, J. A. *Gaussian 98*, Revision A.11; Gaussian, Inc., Pittsburgh, PA, 2001.

(36) Martin, J. M. L.; Bauschlicher, C. W.; Ricca, A. *Comput. Phys. Commun.* **2001**, *133*, 189.

(37) Lynch, B. J.; Fast, P. L.; Harris, M.; Truhlar, D. G. *J. Phys. Chem. A.* **2000**, *104*, 4811.

(38) (a) Parthiban, S.; de Oliveira, G.; Martin, J. M. L. *J. Phys. Chem. A.* **2001**, *105*, 895. (b) Lynch, B. J.; Truhlar, D. G. *J. Phys. Chem. A.* **2001**, *105*, 2936. (c) Iron, M. A.; Lo, H. C.; Martin, J. M. L.; Keinan, E. *J. Am. Chem. Soc.* **2002**, *124*, 7041.

(39) Dolg, M. In *Modern Methods and Algorithms of Quantum Chemistry*; Grotendorst, J., Ed.; John von Neumann Institute for Computing: Jülich, 2000; Vol. 1, pp 479−508.

(40) Dunning, T. H., Jr. *J. Chem. Phys.* **1989**, *90*, 1007.

(41) Martin, J. M. L.; Sundermann, A. *J. Chem. Phys.* **2001**, *114*, 3408.

(42) Sundermann, A.; Uzan, O.; Milstein, D.; Martin, J. M. L. *J. Am. Chem. Soc.* **2000**, *122*, 7095.

(43) Sundermann, A.; Uzan, O.; Martin, J. M. L. *Organometallics* **2001**, *20*, 1783.

(44) Rybtchinski, B.; Oevers, St.; Montag, M.; Vigalok, A.; Rozenberg, H.; Martin, J. M. L.; and Milstein, D. *J. Am. Chem. Soc.* **2001**, *123*, 9064−9077.

out by a two-layer ONIOM[30] approach, in which the *iso*-propyl groups on the phosphorus were placed in the outer layer, and the remainder of the system was placed in the inner layer. For technical reasons, the mPW1k functional was used for both layers. For the inner layer the valence Los Alamos National Laboratory double-ζ (LANL2DZ) basis set- RECP combination was used,[45] whereas for the outer layer, the LANL1MB basis set-RECP combination was employed.[45] (As is customary, first-row atoms in this approach were treated by means of the Dunning−Hay valence double-ζ[46] basis set).

Geometry optimizations for minima were carried out using the standard Schlegel algorithm[47] in redundant internal coordinates until in the neighborhood of the solution, and then continued using analytical second derivatives.[48] Optimizations for transition states were carried out by means of the QST3 approach,[49] with an initial guess for the transition state being generated from either linear synchronous transit (LST[50]) or from manual manipulation of the geometry using MOLDEN.[51] In cases where this approach failed to converge, we used analytical second derivatives at every step.

Where necessary, the Grid = UltraFine combination, i.e., a pruned (99 590) grid in the integration and gradient steps and a pruned (50 194) grid in the CPKS (coupled perturbed Kohn−Sham) steps, was used as recommended in ref 36.

Zero-point and RRHO (rigid rotor-harmonic oscillator) thermal corrections were obtained from the unscaled computed frequencies.

Where necessary to resolve ambiguities about the nature of a transition state, intrinsic reaction coordinate (IRC[52]) calculations were carried out. In some cases where IRC calculation failed for technical reason, displacement along the normal coordinate for the imaginary frequencies and optimizations started from there. Although this procedure is less unambiguous than IRC it at least offers some form of corroboration.

For interpretative purposes, Wiberg bond indices[53] were derived from the natural bond order (NBO) analysis[54] at the mPW1k/SDB-cc-pVDZ level for the H−PCP systems and at the mPW1k/LANL2DZ level for the ^{i}Pr−PCP systems.

The energetics for our final ^{i}Pr−PCP profile were validated by single-point energy calculations, using the ONIOM(mPW1k/LANL2DZ: mPW1k/LANL1MB) reference geometries, at the higher level of theory mPW1k/LANL2DZ+P, where the "+P" stands for the addition of polarization functions with exponents taken from ref 55.

Although the sheer size of the systems studied more or less leaves DFT as the only alternative, DFT has never been really benchmarked for diazo compounds and carbenes. We have therefore considered the reaction energy of

$$(1/2)\ C_2H_4 + N_2 \rightarrow CH_2NN$$

From the respective experimental heats of formation at 298 K of 12.52 ± 0.12 kcal/mol,[56] 0 (by definition), and 49.3 ± 2.3 or 51.3 kcal/mol,[57] we obtain a reaction energy of 43−45 kcal/mol. At the mPW1K/SDB-cc-pVDZ level used in this study, we obtain 51.7 kcal/mol at 298 K, and 52.2 kcal/mol at absolute zero. As the experimental heat of formation for diazomethane would appear to be quite uncertain and the systems are small enough for ab initio computational thermochemistry, we have recalculated the reaction energy using G3X theory[58] as well as the CBS-APNO and CBS-QB3 methods,[59] all of which have average uncertainties in the 1 kcal/mol range for molecular atomization energies, as well as the rather more elaborate W1 and W2h methods[60] which generally achieve sub-kcal/mol accuracy. At absolute zero, we obtain the following reaction energies: G3 × 57.9, CBS-APNO 57.4, CBS-QB3 57.4, W1 58.6, and W2h 58.8 kcal/mol. In other words, five computational thermochemistry methods from three very different families yield fundamentally the same conclusion, namely that the experimental heat of formation of diazomethane is in error by 12−15 kcal/mol: The most accurate (and computationally demanding) method, W2h theory, predicts heats of formation at 0 and 298 K of 66.4 and 65.0, respectively. (For comparison, the same level of theory reproduces the experimental atomization energies of C_2H_4 and N_2 to within 0.45 and 0.32 kcal/mol, respectively. We note that W2h theory is devoid of parameters derived from experiment.)

For the study at hand, this means that the mPW1K/SDB-cc-pVDZ level of theory overestimates the reaction energy by 5−6 kcal/mol. We considered larger basis sets (up to cc-pVQZ[40]) as well as different exchange-correlation functionals (such as B3LYP and B97−1[61]) and obtained qualitatively similar results. For example, at the B97−1/cc-pVQZ level, we obtain a reaction energy of 49.5 kcal/mol at room temperature and 49.9 kcal/mol at absolute zero. As B97−1/TZ2P reproduces the atomization energies of C_2H_4, N_2, and even singlet CH_2 to within 1 kcal/mol,[62] this suggests that diazomethane and similar systems present special difficulties to DFT methods, and we shall investigate this methodological issue in detail soon. Yet the mPW1K/SDB-cc-pVDZ results should still be of sufficient accuracy to permit insight into the reaction mechanism.

Experimental Methods

All experiments with metal complexes and phosphine ligands were carried out under an atmosphere of purified nitrogen in an MBraun MB 150B−G and Vacuum Atmospheres Nexus System gloveboxes. PCP[63] and PCN[64] ligands, $[Rh(COE)_2Cl]_2$[65] and $PhCHN_2$[66] were prepared according to literature procedures. (COE = cyclooctene).

^{1}H, ^{13}C, ^{31}P, and ^{15}N (in 2D ^{15}N-^{1}H correlation) NMR spectra were recorded at 400.1, 100.6, 162.0, and 40.5 MHz, respectively, at 295 K (if not specified otherwise), using a Bruker Avance-400 NMR spectrometer. Long range 2D^{15}N−^{1}H correlation spectrum was measured using the Bruker standard microprogram GHMBC by an inverse gradient selected experiment using a 5-mm Bruker inverse multinuclear resonance probe with a single-axis (z) gradient coil. ^{1}H NMR and ^{13}C-{^{1}H} NMR chemical shifts are reported in ppm downfield from tetramethylsilane. ^{1}H NMR chemical shifts are referenced to the residual

(45) Hay, P. J.; Wadt, W. R. *J. Chem. Phys.* **1985**, *82*, 270, 284, 299.
(46) Dunning, T. H.; Hay, P. J. In *Modern Theoretical Chemistry*; Schaefer, H. F., III, Ed.; Plenum: New York, 1976; Vol. 3.
(47) Schlegel, H. B. *J. Comput. Chem.* **1982**, *3*, 214, Peng, C.; Ayala, P. Y.; Schlegel, H. B.; Frisch, M. J. *J. Comput. Chem.* **1996**, *17*, 49.
(48) Stratmann R. E.; Burant J. C.; Scuseria G. E.; Frisch M. J. *J. Chem. Phys.* **1997**, *106*, 10 175.
(49) Peng, C.; Schlegel, H. B. *Isr. J. Chem.* **1994**, *33*, 449.
(50) Halgren, T. A.; Lipscomb, W. N. *Chem. Phys. Lett.* **1977**, *49*, 225.
(51) Schaftenaar, G. Molden 3.6, 1999. URL: http://www.cmbi.kun.nl/~schaft/molden/molden.html.
(52) Gonzalez, C.; Schlegel, H. B. *J. Chem. Phys.* **1989**, *90*, 2154; *J. Phys. Chem.* **1990**, *94*, 5523.
(53) Wiberg, K. B. *Tetrahedron* **1968**, *24*, 1083.
(54) Reed, A. E.; Curtiss, L. A.; Weinhold, F. *Chem. Rev.* **1988**, *88*, 899.
(55) Hollwarth, A.; Bohme, M.; Dapprich, S.; Ehlers, A. W.; Gobbi, A.; Jonas, V.; Kohler, K. F.; Stegmann, R.; Veldkamp, A.; Frenking, G. *Chem. Phys. Lett.* **1993**, *208*, 237. Ehlers, A. W.; Bohme, M.; Dapprich, S.; Gobbi, A.; Hollwarth, A.; Jonas, V.; Kohler, K. F.; Stegmann, R.; Veldkamp, A.; Frenking, G. *Chem. Phys. Lett.* **1993**, *208*, 111.
(56) *Thermodynamic Properties of Individual Substances*, 4th ed.; Hemisphere: New York, 1989.
(57) Afeefy, H. Y. Liebman, J. F.; Stein, S. E.; *Neutral Thermochemical Data* in *NIST Chemistry WebBook*, NIST Standard Reference Database Number 69, Linstrom, P. J.; Mallard, W. G.; Eds.; (Gaithersburg: National Institute of Standards and Technology, 2001): http://webbook.nist.gov.
(58) Curtiss, L. A.; Redfern, P. C.; Raghavachari, K.; and Pople, J. A.; *J. Chem. Phys.* **2001**, *114*, 108.
(59) Montgomery, J. A., Jr.; Frisch, M. J.; Ochterski, J. W.; Petersson, G. A.; *J. Chem. Phys.* **1994**, *101*, 5900; Montgomery, J. A., Jr.; Frisch, M. J.; Ochterski, J. W.; Petersson, G. A.; *J. Chem. Phys.* **1999**, *110*, 2822.
(60) Martin, J. M. L.; De Oliveira, G.; *J. Chem. Phys.* **1999**, *111*, 1843; Parthiban, S.; Martin, J. M. L.; *J. Chem. Phys.* **2001**, *114*, 6014.
(61) Hamprecht, F. A.; Cohen. A. J.; Tozer, D. J.; Handy, N. C.; *J. Chem. Phys.* **1998**, *109*, 6264.
(62) Boese, A. D., personal communication.
(63) B. Rybtchinski, Y. Ben-David, D. Milstein *Organometallics* **1997**, *16*, 3786.
(64) Gandelman, M.; Vigalok, A.; Shimon, L. J. W.; Milstein, D. *Organometallics* **1997**, *16*, 3981.
(65) Herde, J. L.; Senoff, C. V.; *Inorg. Nucl. Chem. Lett.* **1971**, *7*, 1029.
(66) Creary, X. *Organic Syntheses*; Wiley: New York, 1990; Collect. Vol. VII, p 438.

hydrogen signal of the deuterated solvents, and in $^{13}C\{^1H\}$ NMR the ^{13}C signal of the deuterated solvents was used as a reference. ^{31}P NMR chemical shifts are reported in ppm downfield from H_3PO_4 and referenced to an external 85% solution of phosphoric acid in D_2O. ^{15}N NMR chemical shifts are reported as referenced downfield to liquid ammonia. Abbreviations used in the description of NMR data are as follows: Ar = aryl, br = broad, dist. = distorted, s = singlet, d = doublet, t = triplet, q = quartet, m = multiplet, and v = virtual. Elemental analysis was performed at Mikroanalytisches Laboratorium, 45470 Mülheim, Germany.

Synthesis of 1. A THF solution (3 mL) of the PCP ligand, 1,3-bis-[(diisopropyl-phosphanyl)-methyl]-benzene, (142 mg, 0.419 mmol) was added to a THF solution (5 mL) of $[Rh(COE)2Cl]_2$ (150 mg, 0.209 mmol). The reaction mixture was kept at room temperature for 1 h and dried under vacuum. The residue was dissolved in THF (5 mL) and a THF solution (4 mL) of KOtBu (70 mg, 0.624 mmol) was added to it, resulting in a color change from orange to brown. The reaction mixture was kept for 0.5 h at room temperature, after which the solvent was removed under vacuum and the residue was washed with a small amount of pentane. The resulting solid was extracted with toluene, and the solution was filtered to remove insoluble inorganic particles and dried under vacuum, resulting in 160 mg (84% yield) of **1** as a brown solid. The compound is essentially clean (95% by NMR), and can be used as is. Complex **1** was further purified by crystalization from a toluene-pentane mixture (8 mL, tol:pen = 1:3, v/v) at −35 °C resulting in orange crystals. They were collected by filtration, washed with cold pentane, and dried under vacuum resulting in 100 mg (52.7% yield) of pure complex **1**. It is slightly soluble in pentane and highly soluble in other organic solvents such as benzene, toluene and THF.

1a: $^{31}P\{^1H\}$ NMR (C_6D_6): 66.20 (d, $^1J_{RhP}$ = 157.9 Hz). ^1H NMR (C_6D_6): 7.13 (br. s, 2H, Ar-*H*), 7.09 (m, 1H, Ar-*H*), 3.03 (vt, 4H, J = 3.8 Hz, Ar−C*H*$_2$−P), 2.03 (m, 4H, P−C*H*$(CH_3)_2$), 1.32 (dist q, J_{PH} = 8.0 Hz, 12H, P−CH(C*H*$_3)_2$), 1.09 (dist q, J_{PH} = 6.4 Hz, 12H, P−CH-(C*H*$_3)_2$). $^{13}C\{^1H\}$-NMR (C_6D_6): 172.22 (dt, $^1J_{RhC}$ = 38.4 Hz, $^2J_{PC}$ = 4.9 Hz, C_{ipso}, Rh−Ar), 152.62 (td, *J* = 13.4 Hz, *J* = 3.2 Hz, Ar), 123.31 (s, Ar), 121.23 (t, *J* = 9.4 Hz, Ar), 35.49 (vtd, J_{PC} = 11.5 Hz, J_{RhC} = 4.2 Hz, Ar-*C*H$_2$−P), 25.83 (vt, J_{PC} = 9.5 Hz, P-*C*H$(CH_3)_2$), 20.34 (vt, J_{PC} = 3.3 Hz, P−CH(*C*H$_3)_2$), 18.88 (s, P−CH(*C*H$_3)_2$). IR (film): 2165 cm^{-1}, $\nu_{N\equiv N}$.

Selected NMR data for **1b**: $^{31}P\{^1H\}$ NMR (C_6D_6): 67.35 (d, $^1J_{RhP}$ = 155.5 Hz). ^1H NMR (C_6D_6): 2.98 (vt, 4H, J = 3.6 Hz, Ar−C*H*$_2$−P), 1.85 (m, 4H, P−C*H*$(CH_3)_2$), 1.18 (dist q, J_{PH} = 8.2 Hz, 12H, P−CH-(C*H*$_3)_2$), 0.98 (dist q, J_{PH} = 6.5 Hz, 12H, P−CH(C*H*$_3)_2$). Elemental analysis of **1b**; Anal. Calcd for $C_{40}H_{70}N_2P_4Rh_2$: C, 52.87; H, 7.76. Found: C, 52.75; H, 7.79.

Synthesis of 2. A THF solution of $NaBH(C_2H_5)_3$ (1M, 0.1 mL) was added to a THF solution (3 mL) of the PCN rhodium methyl chloride[64] (50 mg, 0.1 mmol) (PCN: {3-[(di-*tert*-butyl-phosphanyl)-methyl]-benzyl}-diethyl-amine). The reaction mixture was stirred for 20 min at room temperature, after which it was filtered and the solvent removed under vacuum. The resulting solid was extracted with benzene, and the benzene solution was filtered and dried under vacuum resulting in 45 mg (95%) of **2** as a yellow-brown solid. Complex **2** is slightly soluble in pentane and highly soluble in other organic solvents such as benzene, toluene and THF. The characterization of the dimer **2b** is given as it is the main product at room temperature and below.

2b (integration given for one Rh−PCN unit): $^{31}P\{^1H\}$NMR (toluene-d_8): 99.27 (d, $^1J_{RhP}$ = 217.4 Hz). ^1H NMR (toluene-d_8): 6.45 (s, 1H, Ar), 3.79 (s, 2H, Ar−C*H*$_2$−N), 3.08 (dq, $^3J_{HH}$ = 7.2 Hz, $^2J_{HH}$ = 12.3 Hz, 2H, CH_3−C*H*$_2$−N), 2.96 (d, $^2J_{PH}$ = 8.36 Hz, 2H, Ar−C*H*$_2$−P), 2.79 (ddq, $^3J_{HH}$ = 7.0 Hz, $^2J_{HH}$ = 12.1 Hz, $^3J_{RhH}$ = 2.7 Hz, 2H, CH_3−C*H*$_2$−N), 2.23 (s, 3H, Ar−C*H*$_3$), 2.09 (s, 3H, Ar−C*H*$_3$), 1.50 (t, J_{HH} = 7.2 Hz, 6H, C*H*$_3$−CH_2−N), 1.33 (d, $^3J_{PH}$ = 12.3 Hz, 18H, (C*H*$_3)_3$C−P). $^{13}C\{^1H\}$NMR (toluene-d_8): 174.72 (dd, $^1J_{RhC}$ = 29.8 Hz, $^2J_{PC,cis}$ = 3.6 Hz, C_{ipso}, Rh−Ar), 147.81 (s, Ar), 146.83 (s, Ar), 146.25 (d, J_{PC} = 7.1 Hz, Ar), 127.01 (s, Ar), 126.13 (s, Ar), 64.46 (s, Ar-*C*H$_2$−N), 56.18 (s, CH3-*C*H$_2$−N), 34.81 (dd, $^1J_{PC}$ = 15.1 Hz, $^2J_{RhC}$ = 1.6 Hz, $(CH_3)_3C$-P), 30.28 (d, $^2J_{PC}$ = 5.9 Hz, (*C*H$_3)_3$C−P), 21.78 (s, *C*H$_3$−Ar), 13.47 (s, *C*H$_3$−CH_2−N). Assignment of $^{13}C\{^1H\}$NMR signals was confirmed by ^{13}C DEPT. ^{15}N NMR of **2b** labeled with $^{15}N_2$ (toluene-d_8): 305.5 (br d) $^1J_{RhN}$ = 18.4, Rh-*N*≡*N*).

Preparation of the Rhodium Carbene Complex 3. When a C_6D_6 solution of phenyldiazomethane (98 μL, 0.45M solution) was added to a C_6D_6 solution (0.5 mL) of the dinitrogen complex **1** (20 mg, 0.044 mmol of monomer form) at room-temperature quantitative formation of complex **3** accompanied by N_2 evolution was observed. The characterization of compound **3** was reported.[27]

Formation of 4. A C_6D_6 solution of phenyldiazomethane (196 μL, 0.45M solution) was added at −70 °C to a toluene-d_8 solution (0.5 mL) of **1** (40 mg, 0.088 mmol of monomer form), resulting in the quantitative formation of **4**. Complex **4** was characterized in solution at −60 °C.

$^{31}P\{^1H\}$-NMR (toluene-d_8): 66.46 (d, $^1J_{RhP}$ = 154.4 Hz). ^1H NMR (toluene-d_8): 7.31 (m, 1H, Ar-*H*), 7.21 (m, 2H, Ar-*H*), 7.10 (br s, 2H, Ar-*H*), 6.87 (m, 2H, Ar-*H*), 6.53 (m, 1H, Ar-*H*), 3.76 (s, 1H, N_2C*H*Ph), 2.96 (br s, 4H, Ar−C*H*$_2$−P), 1.82 (m, 4H, P−C*H*$(CH_3)_2$), 1.23 (dist q, J_{PH} = 7.4 Hz, 12H, P−CH(C*H*$_3)_2$), 0.98 (dist q, J_{PH} = 6.2 Hz, 12H, P−CH(C*H*$_3)_2$). $^{13}C\{^1H\}$-NMR (toluene-d_8): 173.02 (dt, $^1J_{RhC}$ = 38.3 Hz, $^2J_{PC}$ = 4.9 Hz, C_{ipso}, Rh−Ar), 151.80 (t, J_{PC} = 12.5 Hz, Ar), 132.41 (s, Ar), 126.77 (s, Ar), 123.63 (s, Ar), 122.98 (s, Ar), 121.09 (t, J_{PC} = 9.5 Hz, Ar), 120.56 (s, Ar), 57.95 (s, N_2*C*HPh), 34.80 (vt, J_{PC} = 9.8 Hz, Ar-*C*H$_2$−P), 25.20 (vt, J_{PC} = 9.4 Hz, P-*C*H$(CH_3)_2$), 19.60 (s, P−CH(*C*H$_3)_2$), 18.65 (s, P−CH(*C*H$_3)_2$). The assignment of the ^{13}C-$\{^1H\}$ NMR signals was confirmed by ^{13}C DEPT. ^{15}N NMR from ^{15}N-^1H correlation (toluene-d_8): 421.77 (d, $^1J_{RhN}$ = 31.5 Hz, Rh-*N*≡NCHPh), 300.03 (s, Rh−N≡*N*CHPh).

Preparation of the Rhodium Carbene Complex 5. Addition of a C_6D_6 solution of phenyldiazomethane (93 μL, 0.45M) to a C_6D_6 solution (0.5 mL) of the dinitrogen complex **2** (20 mg, 0.042 mmol of monomer form) at room-temperature resulted in quantitative formation of complex **5** accompanied by N_2 evolution. The characterization of the compound **5** was reported.[27]

Formation of 6. A C_6D_6 solution of phenyldiazomethane (93 μL, 0.45M) was added at −70 °C to a toluene-d_8 solution (0.6 mL) of **2** (20 mg, 0.042 mmol of the monomer form), resulting in the quantitative formation of **6**. Complex **6** was characterized in solution at −70 °C.

$^{31}P\{^1H\}$NMR (toluene-d_8): 88.90 (d, $^1J_{RhP}$ = 204.6 Hz). ^1H NMR (toluene-d_8): 7.49−7.35 (m, 2H, Ar), 6.93 (t, $^3J_{HH}$ = 7.2 Hz, 1H), 6.82 (t, $^3J_{HH}$ = 7.6 Hz, 1H), 6.67 (s, 1H, aromatic proton of the PCN ligand), 6.46 (d, J_{HH} = 8.2 Hz, 1H, Ar), 3.84(s, 1H, N_2C*H*Ph), 3.72−3.48 (multiplets, 4H, Ar−C*H*$_2$−N, Ar−C*H*$_2$−P), 3.18 (ddq, $^3J_{HH}$ = 7.4 Hz, $^2J_{HH}$ = 11.7 Hz, $^3J_{RhH}$ = 2.3 Hz, 2H, CH_3−C*H*$_2$−N), 2.64 (m, 2H, CH_3−C*H*$_2$−N), 2.22 (s, 3H, Ar−C*H*$_3$), 2.00 (s, 3H, Ar−C*H*$_3$), 1.53 (t, J_{HH} = 6.9 Hz, 6H, C*H*$_3$−CH_2−N), 1.16 (d, $^3J_{PH}$ = 12.5 Hz, 18H, (C*H*$_3)_3$C−P). $_{13}C\{^1H\}$NMR (toluene-d_8): 169.52 (dd, $^1J_{RhC}$ = 39.8 Hz, $^2J_{PC,cis}$ = 4.2 Hz, C_{ipso}, Rh−Ar), 150.41 (bs,Ar), 148.1 (d, J_{PC} = 14.1 Hz, Ar), 147.25 (s, Ar), 136.3 (s, Ar), 127.83 (s, Ar), 124.11 (s, Ar), 123.24 (s, Ar), 121.50 (s, Ar), 121.12 (s, Ar), 68.89 (s, N_2*C*HPh), 64.62 (s, Ar-*C*H$_2$−N), 55.40 (s, CH3-*C*H$_2$−N), 36.10 (d, $^1J_{PC}$ = 15.8 Hz, Ar-*C*H$_2$−P), 34.51 (d, $^1J_{PC}$ = 14.5 Hz, $(CH_3)_3C$-P), 30.99 (bs, (*C*H$_3)_3$C−P), 25.70 (s, *C*H$_3$−Ar), 22.15 (s, *C*H$_3$−Ar), 14.96 (s, *C*H$_3$−CH_2−N).

Competition Experiments. In a typical experiment, complex **6** was obtained as described before from complex **2** (15 mg, 0.0315 mmol) and an equimolar amount of $PhCHN_2$ (0.45M C_6D_6 solution) in toluene-d_8. A toluene-d_8 solution of **1** (30 mg, 0.066 mmol) was added at −70 °C to a toluene-d_8 solution of **6** in an NMR tube equipped with rubber septum. The NMR tube was placed in the NMR probe pre-cooled to −70 °C and the reaction was followed at various temperatures.

X-ray Structural Analysis of Complex 1b. Complex **1b** was crystallized from toluene-pentane (1:5, v/v) solution of **1** in C_2/c space group with half a dimer (PCP−Rh−N) per asymmetric unit.

Crystal Data. ($C_{20}H_{35}NP_2Rh$), yellow prisms, 0.2 × 0.2 × 0.1 mm^3, monoclinic, *C*2/*c* (no. 15), $a = 21.628(4)$ Å, $b = 10.970(2)$ Å, $c = 20.463(4)$ Å, $\beta = 112.08(3)°$, from 10 degrees of data, $T = 120$ (2) K, $V = 4499.0(16)$ $Å^3$, $Z = 8$, $F_w = 454.34$, $D_c = 1.342$ Mg/m^3, $\mu = 0.904$ mm^{-1}.

Data Collection and Treatment. Nonius KappaCCD diffractometer, MoKα ($\lambda = 0.71073$ Å), graphite monochromator, 36758 reflections, $-27 \le h \le 25$, $0 \le k \le 13$, $0 \le l \le 25$, frame scan width = 1.4°, scan speed 1° per 70 s, typical peak mosaicity = 0.41°, 4762 independent reflections ($R_{int} = 0.071$). Data were processed with Denzo-Scalepack.

Solution and Refinement. The structure was solved by direct methods with SHELXS-97, and refined by full matrix least-squares based on F^2 with SHELXL-97 (225 parameters with no restraints). Idealized hydrogen atoms were placed and refined in riding mode. The final *R*-factors are $R_1 = 0.029$ (based on F^2) for data with $I > 2\sigma(I)$, and $R_1 = 0.045$ on all 4762 reflections. The goodness-of-fit on F^2 is 1.051, and the largest electron density equals 0.411 e/$Å^3$.

Acknowledgment. This work was supported by the Israel Science Foundation (Grant No 83/00), the MINERVA foundation, Munich, Germany, the Tashtiyot program of the Ministry of Science (Israel), the Israel Inter-University Computing Center and the Helen and Martin Kimmel Center for Molecular Design. We thank Dr. Leonid Konstantinovsky for the help with NMR measurements and Mr. Yehoshoa Ben-David for technical assistance. We also thank Mr. Mark Iron for valuable discussions. D. M. holds the Israel Matz Professorial Chair in Organic Chemistry. B. R. and M. G. are the recipients of The International Precious Metals Institute Student Awards, grants of which supported this work.

Supporting Information Available: X-ray data for **1b** and XYZ coordinates of all computed structures (PDF). This material is available free of charge via the Internet at http://pubs.acs.org.

JA028923C